~~CONFIDENTIAL~~

Copy 6
RM E56G13

UNCLASSIFIED

c.2

RESEARCH MEMORANDUM

THERMODYNAMIC STUDY OF AIR-CYCLE AND MERCURY-VAPOR-CYCLE SYSTEMS FOR REFRIGERATING COOLING AIR FOR TURBINES OR OTHER COMPONENTS

By Alfred J. Nachtigall, John C. Freche, and Jack B. Esgar

Lewis Flight Propulsion Laboratory
Cleveland, Ohio

CLASSIFIED DOCUMENT

This material contains information affecting the National Defense of the United States within the meaning of the espionage laws, Title 18, U.S.C., Secs. 793 and 794, the transmission or revelation of which in any manner to an unauthorized person is prohibited by law.

NATIONAL ADVISORY COMMITTEE FOR AERONAUTICS

WASHINGTON

October 10, 1956

~~CONFIDENTIAL~~

UNCLASSIFIED

NACA RM E56G13

NATIONAL ADVISORY COMMITTEE FOR AERONAUTICS

RESEARCH MEMORANDUM

THERMODYNAMIC STUDY OF AIR-CYCLE AND MERCURY-VAPOR-CYCLE SYSTEMS FOR REFRIGERATING COOLING AIR FOR TURBINES OR OTHER COMPONENTS

By Alfred J. Nachtigall, John C. Freche, and Jack B. Esgar

SUMMARY

A thermodynamic study was made of air-cycle and mercury-vapor-cycle refrigeration devices to evaluate these methods of refrigerating air bled from gas-turbine engine compressors. The study was of a general nature, and the results are presented in dimensionless groupings of terms so that the use of the systems can be evaluated for a wide number of applications.

It appears that for system compressor and turbine efficiencies of about 0.70 the air cycle may hold promise as a refrigeration device if values of heat-exchanger effectiveness on the order of 0.8 or higher can be used. For lower efficiencies or lower values of heat-exchanger effectiveness and for the case where it is possible to have a heat sink at a temperature lower than that of compressor bleed air, a simple heat exchanger is generally capable of refrigerating the bleed air as much or more than the air cycle.

A system employing a mercury-vapor cycle appears feasible for refrigerating air that must enter the system at temperature levels of approximately 1500° R, and this cycle is more efficient than the air cycle. Although the weight of such a device must be considered to determine its effect on specific engine weight, a weight analysis was not included in this thermodynamic study.

INTRODUCTION

This report presents a thermodynamic study of systems for refrigerating air for cooling purposes. High-altitude supersonic flight with turbojet-powered aircraft can introduce cooling requirements in the various engine components and accessories as well as in the pilot's compartment. When air is the coolant, it is usually desirable to use the lowest-temperature air available so as to minimize the quantity needed to maintain an endurable temperature. The pressure level of this air must be high enough to overcome duct losses and the pressure in the coolant

discharge region. Although ram air is the lowest-temperature air available on an aircraft, this pressure requirement may preclude its use as the primary coolant. The alternative is to bleed interstage air from the engine compressor at the required pressure level. If the bleed-air temperature associated with this pressure is too high, it becomes necessary to employ a device for refrigerating the bleed air. The lower air temperature thus obtained permits a reduction in the quantity of air needed for cooling and may at the same time reduce the required pressure.

Numerous studies have been made of various vapor-cycle and air-cycle refrigeration methods (refs. 1 to 3). The emphasis in most of these studies has been on supplying a relatively small amount of air at low temperatures for cabin refrigeration or similar application. The vapor cycles have considered refrigerants in the Freon class, where the maximum operation temperature must be considerably less than 1000° R because of the refrigerant properties. A vapor cycle using a refrigerant capable of operation at temperatures in excess of 1500° R would be of interest for a turbine cooling-air refrigeration method. The air-cycle systems have not been generalized to the point where they can be readily compared with vapor cycles or aftercoolers for wide ranges of temperatures, heat-exchanger effectiveness, and heat-exchanger pressure-loss ratios.

Analytical investigations have also been conducted at the NACA Lewis laboratory to evaluate the general cooling characteristics of various liquid- and air-cooling systems for turbines (refs. 4 and 5, respectively). These studies considered turbine cooling systems applied to an interceptor mission at Mach numbers up to 2.5, an altitude of 50,000 feet, and a turbine-inlet temperature of 2040° F (2500° R). The systems investigated utilized heat rejection to primary burner fuel, to afterburner fuel, and to primary burner-inlet air. In all cases the turbine cooling air was bled from the compressor discharge prior to refrigeration by any of several devices. Although the studies were incomplete in that the refrigeration cycles were not generalized to cover conditions other than the design points considered, and some effects such as heat-exchanger effectiveness and pressure losses were neglected, the study did indicate that compressor bleed air can be refrigerated sufficiently so that it will be useful for cooling various engine components and accessories for flight Mach numbers up to at least 2.5.

Studies such as those in references 6 and 7 have investigated the design of heat exchangers for use in compressor bleed-air refrigeration. A number of liquid-cooling systems for turbines in which the heat is rejected to the engine air at various locations with respect to the engine compressor are described in reference 8, and the effects of this heat rejection on turbojet- and turboprop-engine performance are also discussed.

A generalized study of various types of air refrigeration devices in which the air temperature reduction, the power, and the heat-exchanger

requirements are all presented on a comparable basis would be useful to evaluate the system best suited for a given application. The purpose of this investigation is to present this generalized study for the cases where (1) heat from the air is rejected to a cooler fluid in a heat exchanger, (2) the air is cooled by air-cycle refrigeration (several variations of the cycle are included), and (3) the air is cooled by mercury-vapor-cycle refrigeration. All the systems are compared on the basis of no pressure change across the entire system, but pressure losses within the system such as result from component inefficiencies and heat-exchanger pressure losses are considered. Although these systems were primarily considered for refrigeration of turbine cooling air, the results are so presented that they will be useful for practically any application of an air refrigeration device in which there is no pressure change required across the entire system. An indication is also given of the approximate effect of the power requirements for these refrigeration systems on turbojet-engine performance for flight Mach numbers of 2.5 and 3 and for a turbine-inlet temperature of 2500° R.

METHOD OF ANALYSIS

Basis of Analysis and Assumptions

In order to present the results of several air refrigeration systems so that they can be generalized to cover wide ranges of temperatures and pressure losses, it is desirable to obtain expressions for these results in dimensionless form. In addition, it is desirable to present the results of all systems in the same form so that each system can be compared directly. This method of presentation was the goal of the present study. For a basis of comparison, the system outlet pressure was specified equal to the inlet pressure. Pressure losses within the system were made up by compression at the system inlet, and the work required was charged against the system. Pressure losses in the heat-sink fluid were neglected, however.

Evaluation of systems where constant pressure across the system is not specified can often be misleading. Such systems can show substantial temperature reductions across the system; however, part of this temperature reduction is obtained by utilizing the pressure ratio across the system. This pressure ratio is the result of excess pressure at the system inlet. Unless the system outlet temperature is less than the temperature associated with a bleed source where the pressure is equal to the system outlet pressure, no real refrigeration is accomplished.

Two main types of refrigeration systems were analyzed: (1) air-cycle refrigeration using a compressor, heat exchanger, and expansion turbine; and (2) mercury-vapor-cycle refrigeration. Several other systems can be evaluated as special cases of these main systems.

The heat sink is not specified in this general analysis. The receiver fluid in the sink can be either gas or liquid and can be at temperatures either higher or lower than the system inlet-air temperature. For an aircraft engine, possible heat sinks may be ram air, engine compressor-discharge air, fuel, or an expendable vaporizing fluid.

In making an analysis general, the question arises whether the analysis should be made with constant or variable specific heat and, if constant, what value should be used. A preliminary error analysis was therefore conducted on the air and vapor cycles to determine specific-heat effects. By assuming a mean value of the ratio of specific heats of 1.38, corresponding to a specific heat at constant pressure of 0.249 Btu/(lb)($^{\circ}$R), the maximum error in work amounted to about $2\frac{1}{2}$ percent and the maximum error in outlet temperature to about 1 percent for a range of inlet temperatures T_1 from 550° to 1500° R and compressor pressure ratios up to 10 for the air cycle. For the mercury-vapor cycle, errors up to 3 percent can occur in the outlet temperature for low inlet temperatures; this error will not exceed 10° R, however. No improvement in accuracy over a range of inlet temperatures was found when variable specific heat calculations were made for a mean value of inlet temperature. The errors introduced in this analysis are a function of temperature level more than of temperature change through the cycle. Based on this error analysis, a mean value of 1.38 was used for the ratio of specific heats for all the cycles investigated.

5014

Air-Cycle Refrigeration

General analysis. - A generalized system for the air cycle is shown in figure 1. The auxiliary-compressor and -turbine units may be free-running or mechanically coupled to the engine shaft. The sketch and numbering system for the stations are arranged so that a single analysis of the system can be used for a number of cycle variations. For refrigeration systems used in aircraft engines, the main engine compressor will undoubtedly be used for part of the air-cycle compression process. For illustrative purposes, therefore, the main compressor is shown divided into two parts in figure 1. Station 1 can be considered as the location on the compressor where the air pressure is the same as the required pressure at station 5.

Any work done on the bleed air in the compressor beyond station 1 should therefore be charged against the air-cycle refrigeration system. The compression occurring between stations 2 and 3 is beyond the capabilities of the main engine compressor. For the general analysis the compression occurring between stations 1 and 3 can be considered to take place in a single compressor, and the total system power $\mathscr{P}_t$ will be the sum of $\mathscr{P}_{1-2}$ plus $\mathscr{P}_{2-5}$.

The symbols used in the derivation of all equations are given in appendix A. The derivations of all equations for the air cycle are given in appendix B. A generalized expression involving only dimensionless groupings of terms can be written to relate the power required for an air cycle to obtain a given cycle temperature ratio for any given compressor pressure ratio:

$$\eta_{C,a}\eta^{*}\psi\,\frac{T_5}{T_1} = 1 - \frac{\eta_{C,a}\left(\frac{\mathscr{P}_t}{w_a c_{p,a} T_1}\right)}{\left(\frac{P_3}{P_1}\right)^{\frac{\gamma-1}{\gamma}} - 1} \tag{1}$$

where $\eta_{C,a}$ is the adiabatic efficiency of the entire cycle compression process from stations 1 to 3. The term η^* is a fictitious turbine efficiency that can be related to the adiabatic turbine efficiency η_T by the relation

$$\eta^{*} \equiv \frac{\eta_T\left[1 - \left(\frac{P_5}{P_4}\right)^{\frac{\gamma-1}{\gamma}}\right]}{\left\{1 - \eta_T\left[1 - \left(\frac{P_5}{P_4}\right)^{\frac{\gamma-1}{\gamma}}\right]\right\}\left[\left(\frac{P_4}{P_5}\right)^{\frac{\gamma-1}{\gamma}} - 1\right]} \tag{2}$$

The term ψ is related to the heat-exchanger pressure ratio by

$$\psi \equiv \frac{\left(\frac{P_3}{P_1}\frac{P_4}{P_3}\right)^{\frac{\gamma-1}{\gamma}} - 1}{\left(\frac{P_3}{P_1}\right)^{\frac{\gamma-1}{\gamma}} - 1} \tag{3}$$

Equations (1), (2), and (3) are presented in graphical form in figures 2, 3, and 4, respectively.

Although equation (1) is mathematically correct, a specified amount of heat must be rejected to a heat sink before the temperature ratio T_5/T_1 can be obtained. The heat that is rejected can be expressed in terms of the heat-exchanger effectiveness ε_h, the temperature ratio

T_R/T_1, and the system compressor pressure ratio P_3/P_1. The temperature ratio that can be obtained for given values of P_3/P_1, ε_h, and T_R/T_1 is

$$\frac{T_5}{T_1} = \frac{\left\{\frac{1}{\eta_{C,a}}\left[\left(\frac{P_3}{P_1}\right)^{\frac{\gamma-1}{\gamma}} - 1\right] + 1\right\}(1 - \varepsilon_h) + \varepsilon_h \frac{T_R}{T_1}}{\eta^* \psi \left[\left(\frac{P_3}{P_1}\right)^{\frac{\gamma-1}{\gamma}} - 1\right] + 1} \tag{4}$$

The term ε_h used in equation (4) is defined as

$$\varepsilon_h = \frac{T_3 - T_4}{T_3 - T_R} \tag{5}$$

The basic definition of heat-exchanger effectiveness considers the right side of equation (5) to be multiplied by the ratio $\frac{(wc_p)_a}{(wc_p)_{min}}$, where $(wc_p)_{min}$ is the smaller product of weight flow and specific heat of the two fluids engaged in heat exchange. Thus, to convert a basic heat-exchanger effectiveness $\mathscr{E}$ to the effectiveness term employed in this analysis, the following equation may be used:

$$\varepsilon_h = \frac{T_3 - T_4}{T_3 - T_R} = \mathscr{E} \frac{(wc_p)_{min}}{(wc_p)_a} \tag{6}$$

By a combination of equations (1) and (4) the characteristics of an air-cycle refrigeration system can be determined. For specific values of component efficiencies and heat-exchanger pressure losses and effectivenesses, the combination of the two equations can be used to make plots showing the temperature ratio T_5/T_1 obtained and the power parameter $\mathscr{P}_t/w_a c_{p,a} T_1$ required for a system with any compressor pressure ratio P_3/P_1 and ratio of receiver fluid temperature to inlet-air temperature T_R/T_1.

Free-running compressor and turbine system. - For a refrigeration application where there is a source of high-pressure air, such as in a gas-turbine engine, it is not always necessary to have a source of power external to the refrigeration cycle to drive the auxiliary compressor shown between stations 2 and 3 (fig. 1). The power from the auxiliary (expansion) turbine is sufficient for driving an auxiliary compressor

with some pressure ratio. Hereinafter this type of system will be referred to as a free-running system. The general equations (1) to (4) are still valid for this air cycle, but an additional relation is required to specify the auxiliary-compressor pressure ratio P_3/P_2 that results when the power from the auxiliary turbine is exactly equal to that required to drive the auxiliary compressor:

$$\frac{P_3}{P_2} = \left\{ 1 + \frac{\eta_{C,a}\eta^*\psi \frac{T_5}{T_1}\left[\left(\frac{P_3}{P_1}\right)^{\frac{\gamma-1}{\gamma}} - 1\right]}{1 + \frac{\mathscr{P}_t}{w_a c_{p,a} T_1}} \right\}^{\frac{\gamma}{\gamma-1}} \tag{7}$$

Aftercooler system. - For the case with the simple aftercooler, the auxiliary turbine is eliminated and the only purpose of the compressor is to overcome the pressure loss in the heat exchanger so that there will be no pressure change across the entire system. Such a system can be evaluated by letting

$$\frac{P_3}{P_1} = \frac{1}{P_4/P_3} \tag{8}$$

The power required for the cycle can then be calculated from equation (1) with the left side of the equation equal to zero. The power is independent of the temperature ratio T_5/T_1 in this case. The temperature ratio T_5/T_1 can be calculated from equation (4), which for this special case becomes

$$\frac{T_5}{T_1} = \left\{ \frac{1}{\eta_{C,a}}\left[\left(\frac{P_3}{P_1}\right)^{\frac{\gamma-1}{\gamma}} - 1\right] + 1 \right\}(1 - \varepsilon_h) + \varepsilon_h \frac{T_R}{T_1} \tag{4a}$$

Variables investigated. - The following range of variables for the air-cycle system was investigated:

System compressor pressure ratio, P_3/P_1	1 to 10
System compressor adiabatic efficiency, $\eta_{C,a}$	0.50 to 0.80
Auxiliary-turbine adiabatic efficiency, η_T	0.50 to 0.80
Heat-exchanger effectiveness, ε_h	0.50 to 1.0
Heat-exchanger pressure ratio, P_4/P_3	0.90 to 1.0
Ratio of receiver to system inlet-air temperature, T_R/T_1	0.6 to 1.2

[redacted]

The presentation of results becomes impractical if too many variables are considered together. Consequently, most of the results are presented for compressor and turbine efficiencies of 0.70, heat-exchanger effectiveness values of 0.6 to 0.8, and an heat-exchanger pressure ratio of 0.95. These are probably practical values for the size of components that would be involved in refrigeration systems. Variations in these variables were investigated for compressor pressure ratios of 1/0.95, 2.5, 5, and 10 for T_R/T_1 of 0.6 and 1.0.

Mercury-Vapor-Cycle Refrigeration

The mercury-vapor cycle is shown schematically in figure 5. The system operates on the same principle as the household mechanical refrigerator. However, the choice of refrigerants for operation at high temperatures is very limited. The data on the thermodynamic properties of mercury (enthalpy, entropy, and density) for the desired temperature range are suitable and readily available for refrigerant temperatures up to at least 1800° R; consequently, mercury was considered as being a likely refrigerant (ref. 9). In this system the air to be refrigerated is passed through an evaporator, where it is cooled by rejecting heat to the refrigerant. Heat absorbed by the refrigerant is transported to the condenser, where this quantity of heat plus the work of compression is rejected. The heat-receiving fluid could be one of the same fluids indicated for the air cycle. The thermodynamic cycle of the refrigerant shown by the enthalpy-entropy diagram in figure 6 is discussed in appendix C.

In order to compare the mercury-vapor cycle on the same basis as the air cycle, that is, system outlet pressure equal to system inlet pressure, for the refrigerated air, it is necessary to compress the air enough to overcome pressure losses in the evaporator. This compression process affects both the air temperature-reduction ratio and the power requirements of the system. The temperature change and power requirements of the compression process must be combined with those of the mercury-vapor cycle to fully evaluate the system. The power parameter and air temperature-reduction ratio in the mercury-vapor cycle can be related by the following equation derived in appendix C:

$$\frac{T_4}{T_3} = 1 - \frac{\mathscr{P}_r}{w_a c_{p,a} T_3}\left\{\left[\frac{\eta_{C,r}(H_{v,y} - H_{l,z})}{\frac{(S_{v,y} - S_{v,x})(H_{v,x} - H_{l,x})}{S_{l,x} - S_{v,x}} + (H_{v,y} - H_{v,x})}\right] - 1\right\} \tag{9}$$

In the mercury-vapor cycle the refrigerant temperatures are assumed to be constant through the condenser and also through the evaporator. That is, evaporation and condensation take place at the saturation temperatures

T_e and T_c and their associated pressures specified in the analysis. Temperatures and pressures in the superheated region were not considered. The enthalpy and entropy used in equation (9) were obtained from tables in reference 10.

The total power parameter and the system temperature-reduction ratio for the entire system are also derived in appendix C. The total power parameter for the system is

$$\frac{\mathscr{P}_t}{w_a c_{p,a} T_1} = \left(\frac{\mathscr{P}_r}{w_a c_{p,a} T_3} + 1\right)\left\{1 + \frac{1}{\eta_{C,a}}\left[\left(\frac{1}{P_4/P_3}\right)^{\frac{\gamma-1}{\gamma}} - 1\right]\right\} - 1 \qquad (10)$$

and the system air temperature-reduction ratio is

$$\frac{T_5}{T_1} = \frac{T_4}{T_3}\left\{1 + \frac{1}{\eta_{C,a}}\left[\left(\frac{1}{P_4/P_3}\right)^{\frac{\gamma-1}{\gamma}} - 1\right]\right\} \qquad (11)$$

where the system compressor pressure ratio is the reciprocal of the heat-exchanger (evaporator) pressure ratio as expressed in equation (8).

The air temperature ratio across the evaporator T_4/T_3 is also related to the heat-exchanger effectiveness of the condenser and evaporator and to the receiver temperature by the following expression:

$$\frac{T_4}{T_3} = \frac{\varepsilon_c \frac{(wc_p)_R}{(wc_p)_a}\left(\frac{1}{\varepsilon_e}\frac{T_c}{T_e} + \frac{T_R}{T_3} - \frac{T_c}{T_e}\right) + 1 - \frac{1}{m}}{\varepsilon_c \frac{(wc_p)_R}{(wc_p)_a}\frac{1}{\varepsilon_e}\frac{T_c}{T_e} + 1 - \frac{1}{m}} \qquad (12)$$

Values of $1/m$ as a function of T_c/T_e are tabulated in appendix C.

The basic definition of heat-exchanger effectiveness is related to the condenser effectiveness used herein by the equation

$$\varepsilon_c = \frac{\frac{(wc_p)_a}{(wc_p)_R}\left[(T_3 - T_4) + \frac{\mathscr{P}_r}{(wc_p)_a}\right]}{T_c - T_R} = \mathscr{E}_c \frac{(wc_p)_{min}}{(wc_p)_R} \qquad (13)$$

[redacted]

and to the evaporator effectiveness used herein by the equation

$$\varepsilon_e = \frac{T_3 - T_4}{T_3 - T_e} = \mathscr{E}_e \frac{(wc_p)_{min}}{(wc_p)_a} \tag{14}$$

The mercury-vapor compression cycle was investigated for the following range of variables and assigned constants:

Evaporator refrigerant temperature, T_e, $^\circ R$	910 to 1210
Condenser refrigerant temperature, T_c, $^\circ R$	1460 to 1760
Refrigerant compressor efficiency, $\eta_{C,r}$	0.5
Air compressor efficiency, $\eta_{C,a}$	0.7
Heat-exchanger (evaporator) pressure ratio, P_4/P_3	0.9 to 1.0

A plot of the power parameter $\mathscr{P}_r/w_a c_{p,a} T_3$ against T_c/T_e for values of T_3/T_4 indicated that, in addition to its effect on the ratio T_c/T_e, T_e had a secondary effect on the power parameter. For values of T_c/T_e below 1.5, this effect was considered small enough that a mean curve for the range of T_e investigated could be used. From such a mean curve, uniform steps in T_c/T_e from 1.1 to 1.5 were selected for further investigation.

In order to evaluate fully the mercury-vapor cycle, equations (9) to (12) must be evaluated simultaneously. Fortunately, these equations can be shown on a single plot for assigned values of the condenser effectiveness parameter $\varepsilon_c \frac{(wc_p)_R}{(wc_p)_a}$ and evaporator effectiveness ε_e.

Effect of Power Extraction on Turbojet-Engine Performance

Air refrigeration systems can cause a number of effects on engine performance. The use of compressor bleed air for turbine cooling results in variations in engine performance, as discussed in reference 11. Additional changes that air refrigeration can cause in engine thrust and specific fuel consumption can result from (1) power extraction to drive the refrigeration system; (2) heat-exchanger drag on the heat-sink side: if heat is rejected to the engine air, the exhaust-nozzle pressure ratio is affected; if heat is rejected to bypass ram air, the effects of taking this air aboard plus the ducting pressure losses and the effect of air discharge must be accounted for; (3) heat addition to the heat sink: the engine fuel consumption will be affected if heat is added to the engine air or fuel. An evaluation of the effects listed under (2) and (3) requires that the over-all refrigerant-system design be known. Once this is established, the heat receiver and its location are specified, and the heat

exchanger can be designed to accommodate the pressure losses which may be encountered. Since these conditions are difficult to generalize, only the effect of power extraction will be studied. This effect was analyzed by the method of reference 12.

The variables and assigned constants in the study of the effect of power extraction on turbojet-engine performance are shown in the following table. The component efficiencies and the pressure losses within the engine were essentially the same as for the engine analyses presented in references 8 and 11.

Flight Mach number, M	2.5 and 3.0
Turbine-inlet temperature, $^{\circ}R$	2500
Engine compressor pressure ratio at flight conditions	2, 4, or 6
Afterburner temperature, $^{\circ}R$	3500
Power extraction term $\mathscr{P}_t/w_E$, Btu/(lb)	0 to 40
Flight altitude	Stratosphere
Engine compressor adiabatic efficiency	0.88
Engine turbine polytropic efficiency	0.85
Primary-combustor efficiency	0.98
Afterburner efficiency	0.90
Exhaust-nozzle efficiency	0.90
Primary-combustor pressure ratio	0.95
Tailpipe and afterburner pressure ratio	0.90
Tailpipe pressure ratio without afterburner	0.99
Ram recovery at M = 2.5	0.75
Ram recovery at M = 3.0	0.65

RESULTS AND DISCUSSION

Air-Cycle Refrigeration

Generalized presentation. - Generalized results of the power requirements for the air-cycle refrigeration system are presented in figure 2. As indicated by equation (1), the temperature-reduction parameter decreases linearly with increasing cycle power parameter for each refrigeration-cycle compressor pressure ratio. For a given value of temperature-reduction parameter, the power parameter increases with increasing cycle compressor pressure ratio. In order to make use of figure 2, it is necessary to know η^* and ψ in terms of the more commonly used parameters (adiabatic turbine efficiency η_T and heat-exchanger pressure drop P_3/P_4). Figure 3 presents the variation of η^* with turbine pressure ratio for four values of η_T (0.5, 0.6, 0.7, and 0.8). The value of η^* decreases with increasing turbine pressure ratio. For a pressure-ratio increase from 1 to 10, the decrease is 15 percent for $\eta_T = 0.80$ and about 31 percent for $\eta_T = 0.50$. The variation of the heat-exchanger pressure-drop parameter ψ with compressor pressure ratio is given in figure 4 for three values of heat-exchanger pressure ratio.

[redacted]

It must be emphasized that figure 2 can only be used to determine the power required to obtain a given temperature-reduction ratio T_5/T_1. The figure cannot be used alone to determine what temperature-reduction ratio is possible. The possible temperature reduction is a function of the heat removed from the cycle and can be expressed in terms of a heat-exchanger effectiveness ϵ_h and the ratio of receiver to cycle inlet temperature T_R/T_1. Further discussion on this heat removal will follow in the subsequent section.

Effect of heat sink on temperature reduction and power. - For an aircraft engine, the temperature level at the inlet to the refrigeration cycle is a function of the flight Mach number as it affects the engine inlet-air temperature through ram and the pressure ratio of the engine compressor up to the inlet of the refrigeration cycle. At flight Mach numbers of about 2.5 or higher, air bled from the engine compressor can easily become too hot to use advantageously as a coolant for engine components or accessories. For cabin pressurization or cooling, the bleed air is probably too hot at all flight speeds. For these conditions a device for refrigerating the bleed air will probably be required.

5014

Figure 7 presents performance plots for air-cycle refrigeration (see fig. 1) for compressor and turbine adiabatic efficiencies of 0.70. This is probably a reasonable value of efficiency for small compressor and turbine components because higher efficiencies are usually found only on larger components such as the main compressor and turbine in turbojet engines. The relation between the system air temperature-reduction ratio T_5/T_1, the air-cycle system compressor pressure ratio P_3/P_1, and the power parameter $\mathscr{P}_t/w_a c_{p,a} T_1$ can be obtained from equation (1) or figure 2. It is important to note and remember that, when any combination of the temperature and power parameters is chosen, the heat that must be rejected from the air cycle to a heat sink is a fixed value. This value of heat rejection can be expressed in terms of the heat-exchanger effectiveness ϵ_h and the ratio of receiver to air-cycle inlet temperature T_R/T_1. The effect of these factors can also be plotted as shown in figure 7. Figure 7(a) is for a heat-exchanger effectiveness of 0.6, and figure 7(b) is for an effectiveness of 0.8. A range of temperature ratios T_R/T_1 from 0.6 to 1.2 is covered. The air cycle is acting as a heat pump only when T_R/T_1 is greater than 1.0. The air cycle is not acting as a refrigeration device when T_5/T_1 is greater than 1.0. Higher values of T_5/T_1 are shown by lighter lines to show trends, but these values are of no practical significance.

Before the significance of figure 7 is discussed, it must also be pointed out that the vertical lines near the ordinate for $P_3/P_1 = 1/(P_4/P_3)$ represent the case where there is no air cycle. This is the aftercooler case, and the compressor pressure ratio is only high enough to overcome the pressure loss in the heat exchanger.

For component efficiencies of 0.70 and a heat-exchanger effectiveness of 0.6 (fig. 7(a)), the air cycle is of absolutely no value. For a given ratio of T_R/T_1, system outlet temperatures T_5 that are equal to or lower than those obtainable with air-cycle systems can be obtained by use of only an aftercooler. A somewhat greater temperature reduction can be obtained with an air cycle than with an aftercooler if the heat-exchanger effectiveness is increased to 0.8 (fig. 7(b)). The advantage of the air cycle over the aftercooler becomes less, however, as T_R/T_1 decreases. With a heat-exchanger effectiveness of 0.8, the cycle can also be used as a heat pump ($T_R/T_1 > 1.0$); this was not possible for an effectiveness of 0.6.

Also shown in figure 7 is the effect of heat-exchanger pressure ratio P_4/P_3 on air-cycle power requirements. The effect is shown for only three compressor pressure ratios, and it consists of displacing the auxiliary-compressor pressure-ratio lines slightly.

The effect of component efficiencies for the air-cycle compressor and turbine is shown in figure 8 for efficiencies of 0.50, 0.60, and 0.80 ($\eta_{C,a} = \eta_T = 0.70$ is shown in fig. 7) for values of heat-exchanger effectiveness of 0.6 and 0.8. In figure 8 and all subsequent figures on the air cycle, the heat-exchanger pressure ratio P_4/P_3 was assumed to be 0.95. As would be expected from figure 7, efficiencies lower than 0.70 would make the air cycle unacceptable for a heat-exchanger effectiveness of 0.6 (figs. 8(d) and (e)). It will be noted from figure 8(a) that the air cycle is also impractical when used with a heat-exchanger effectiveness of 0.8 for component efficiencies of 0.50 and probably impractical for efficiencies of 0.60 (fig. 8(b)). About the only condition shown in figure 8 where the air cycle appears to be promising is for the case where the component efficiencies are 0.80 and the heat-exchanger effectiveness is 0.8 (fig. 8(c)).

Figure 9 shows air-cycle performance for component efficiencies of 0.70 and temperature ratios T_R/T_1 of 0.6 and 1.0 for a range of values of heat-exchanger effectiveness. For either temperature ratio T_R/T_1 the values of heat-exchanger effectiveness of 0.6 or less are impractical because a simple aftercooler system is equally or more effective. At an effectiveness of 0.8, the air cycle is only a slight improvement over the aftercooler for $T_R/T_1 = 0.6$. A higher effectiveness, of course, results in improved air-cycle performance.

Compressor pressure ratios for free-running system. - In using an air cycle where part of the compression can be accomplished in a large compressor such as the main compressor of a gas-turbine engine, it may be desirable to utilize the auxiliary (expansion) turbine power instead

of a source of power external to the cycle to drive an auxiliary compressor. For this case $\mathscr{P}_{2-5} = 0$. Since heat is removed from the air in the heat exchanger prior to passing through the auxiliary turbine (see fig. 1), the power that the turbine can produce is quite limited and the pressure ratio of the auxiliary compressor that the turbine drives will be considerably less than the turbine pressure ratio. The turbine pressure ratio will be the product of P_3/P_1 and P_4/P_3, since it is specified that there is no pressure change across the air cycle and therefore $P_5 = P_1$.

The auxiliary-compressor pressure ratios P_3/P_2 for the case where the auxiliary-turbine power is exactly equal to the auxiliary-compressor power is shown as a parameter in figure 10 for a range of component efficiencies from 0.50 to 0.80. For component efficiencies of 0.60 and lower, the auxiliary-compressor pressure ratio cannot be higher than about 1.4. For component efficiencies of 0.80, the auxiliary-compressor pressure ratio cannot be higher than about 2.2 even for auxiliary-turbine pressure ratios approaching 10. These results indicate that for free-running systems the main purpose of the auxiliary compressor would be as a convenient power-absorption device for the auxiliary turbine. The allowable pressure ratio of the auxiliary compressor could not contribute to an appreciable reduction in the air-cycle outlet temperature.

It should be pointed out that the results presented in figure 10 in no way affect the results presented in figures 7 to 9. Overlays of figures having the same component efficiencies are possible so that the combined effect of heat-exchanger effectiveness, temperature ratio T_R/T_1, and free-running compressor pressure ratio can be observed. In other words, figures 7 to 9 are applicable to both free-running and mechanically coupled systems.

Mercury-Vapor Compression Cycle

A vapor compression refrigeration cycle is of interest because it more nearly approaches the reversed Carnot cycle than the air cycle does. It can therefore be expected to be more efficient and require less power to operate. For the intended application for this type of cycle (refrigerating engine compressor bleed air whose temperature level may be between 1000° to 1500° R) there are few satisfactory refrigerant fluids. As previously mentioned, mercury vapor was chosen for this particular study because its thermodynamic properties make it a suitable refrigerant for this application and the data pertaining to the physical properties of mercury are readily available.

Results of this study are presented in figure 11, which is essentially a combination of three separate plots. The obtainable system air

temperature-reduction ratio is plotted against the power parameter as previously done for the air cycle. The narrow plots of inclined lines attached to the ordinate and abscissa account for the effects of the compressor pressure ratio needed to overcome evaporator pressure drop on cycle temperature ratio (eq. (11)) and cycle power (eq. (10)). The compressor adiabatic efficiency used was 0.7. The principal part of the figure is that bounded by the line for an evaporator pressure ratio of 1.0 on the ordinate and abscissa. The ordinate is the air temperature-reduction ratio T_4/T_3 across the evaporator; the abscissa is the refrigerant compressor power parameter $\mathscr{P}_r/w_a c_{p,a} T_3$ for a compression efficiency of 0.50. The solid lines of constant T_c/T_e represent the parameter within the brackets of equation (9), which is a function of liquid and vapor saturation enthalpies and entropies for the evaporator and condenser temperatures. The parameter within the bracket is primarily a function of the ratio T_c/T_e. The secondary effect of temperature level T_e on the parameter was ignored for this presentation since it was considered negligible for values of T_c/T_e less than or equal to 1.5.

The plot can be read by following the arrows shown in the figure. For example, starting with a desired system air temperature-reduction ratio, read across horizontally to the desired value of evaporator pressure ratio P_4/P_3. Then follow between the adjacent inclined lines, interpolating between them, until the principal ordinate T_4/T_3 is reached. The main plot is then entered horizontally until the desired value of T_R/T_3 or T_c/T_e is reached. From this point proceed vertically downward to the abscissa. The plot of inclined lines along the abscissa is read in a similar manner (only reversed) as that along the ordinate.

The performance plot for the mercury-vapor system is similar to those for the air system in that it must be remembered that any combination of T_5/T_1 and $\mathscr{P}_t/w_a c_{p,a} T_1$ results in a fixed amount of heat that must be rejected from the refrigeration cycle. As a result, the temperature reduction that is possible is a function of the receiver temperature and the heat-transfer characteristics of the condenser and evaporator. By means of equation (12) these effects can be fully evaluated.

In order to show the lowest system air temperature-reduction ratio T_5/T_1 that is possible for a given value of T_R/T_3, dashed lines are included on figure 11 with T_R/T_3 as the parameter. For $\varepsilon_e = 1.0$ and $\varepsilon_c \frac{(wc_p)_R}{(wc_p)_a} = \infty$ (fig. 11(a)), a very substantial system air temperature-reduction ratio (T_5/T_1 less than about 0.7) with the mercury-vapor cycle will probably require a receiver temperature that is colder than the system inlet-air temperature. For T_5/T_1 greater than 0.7, it is possible to use the cycle as a heat pump.

[redacted]

The figure also shows that the use of a condenser-to-evaporator temperature ratio T_c/T_e greater than about 1.3 is generally wasteful of power required to drive the cycle. At higher values, the power generally increases very substantially with only slight additional reductions in system outlet temperature T_5 except for $T_R/T_3 > 1.0$.

Figure 11(b) indicates that with more realistic parameter values $\left(\varepsilon_e = 0.8 \text{ and } \varepsilon_c \frac{(wc_p)_R}{(wc_p)_a} = 4\right)$ the obtainable system outlet temperature T_5 is not as low as shown in figure 11(a). For example, at a constant parameter value of $T_R/T_3 = 0.6$, and a constant power parameter of 0.45, the system air temperature-reduction ratio is 0.47 in figure 11(a) and 0.66 in figure 11(b).

The effects of ε_e and $\varepsilon_c \frac{(wc_p)_R}{(wc_p)_a}$ on air temperature-reduction ratio T_4/T_3 for the cycle are illustrated in figure 12. For simplicity, the ordinate on these plots does not include the effect of air compression required to overcome air pressure drop across the evaporator on temperature as was shown in figure 11. Under the rather wide range of conditions illustrated, the evaporator heat-exchanger effectiveness ε_e and the condenser effectiveness parameter $\varepsilon_c \frac{(wc_p)_R}{(wc_p)_a}$ must be maintained as high as possible in order to obtain low cycle outlet temperatures. For this cycle, it usually will be necessary for the product wc_p for the receiver fluid to be several times (at least 4) as great as wc_p for the air in the cycle in order to obtain appreciable air temperature reductions.

A rough indication of the power requirements for both air and mercury-vapor cycle can be obtained from figures 9(b) and 11(a), respectively, for the ideal cases where the heat exchangers in both cases have the highest possible effectiveness. Using conditions that are duplicated in both curves, it can be seen from figure 9(b) that a system air temperature-reduction ratio T_5/T_1 of 0.85 requires a power parameter of 0.27 for the air cycle. The power parameter required for the mercury-vapor cycle (fig. 11(a)) is 0.11, and it is obtained by following the illustrative line on the figure. It will be noted that for $T_R/T_1 = 1.0$

$$\frac{T_R}{T_3} = (1.0)\ \frac{0.835}{0.85} = 0.982$$

using the equation shown in the figure. The value of T_4/T_3 is read from the ordinate to the right of the inclined lines for a value of $P_4/P_3 = 0.95$.

A comparison of the two systems for more practical values of heat-exchanger effectiveness $\varepsilon_h = \varepsilon_e = 0.8$ can be obtained from figures 9(b) and 11(b) when $\varepsilon_c \frac{(wc_p)_R}{(wc_p)_a} = 4$ for the mercury-vapor system. For a system air temperature-reduction ratio T_5/T_1 of 0.85, the power parameter is now 0.80 for the air cycle and 0.30 for the mercury-vapor cycle. In both examples, the power for the mercury-vapor cycle is less than half of that for the air cycle. Although the savings in power using the mercury-vapor cycle will not necessarily always be of this magnitude, the higher efficiency of the cycle is illustrated. Under some modes of operation where T_c/T_e is high, the mercury-vapor cycle will become less efficient.

From this rather preliminary study of air and mercury-vapor cycles and aftercoolers, these systems are probably feasible for refrigerating air that must enter the system at temperature levels of approximately 1500° R. For the case where the aftercooler is not sufficient for obtaining air temperature reduction, either the air or mercury-vapor cycles could be used, but the mercury-vapor cycle is more efficient. In this study, weight was not considered in evaluating the systems; such a study would be required before the final choice of a system could be made.

Variations and Combinations of Systems

A number of variations to the systems discussed can also be evaluated by using the curves presented herein. Generally this evaluation is made by assuming the over-all system is made up of two or more simpler systems in series and by using the outlet temperature from one system as the inlet temperature for the next system. The total power requirement for the entire system would then be the sum of the powers required for each of the simpler systems.

It was mentioned previously that the aftercooler could be evaluated from the curves presented for the air cycle; the system compressor pressure ratio P_3/P_1 is taken as the reciprocal of the heat-exchanger pressure ratio P_4/P_3. An air-cycle system with an aftercooler both before and after the compression process can be evaluated by assuming the air cycle shown in figure 1 to be in series with an aftercooler. An aftercooler ahead of a mercury-vapor cycle could also be evaluated in a similar manner. Another alternative might be an air cycle in series with a mercury-vapor cycle. However, the charts presented herein cannot be used to evaluate an air cycle with a heat exchanger located at station 2 (fig. 1) for any case except where the pressure ratio P_2/P_1 is the reciprocal of the heat-exchanger pressure ratio.

[redacted]

Effects of Refrigeration Systems on Turbojet-Engine Performance

As indicated earlier, the effects of engine shaft power extraction were studied for a turbojet engine with a turbine-inlet temperature of 2500° R at flight Mach numbers of 2.5 and 3.0 for engine operation with and without afterburning. The afterburning temperature was 3500° R. Engine compressor pressure ratios of 2, 4, and 6 at flight conditions were studied. The shaft power extraction parameter $\mathscr{P}_t/w_E$ was varied from 0 to 40 Btu per pound of engine air. The results of this study are presented in figure 13. From this figure it is evident that the nonafterburning engine is more sensitive to the effects of shaft power extraction at both flight speeds but is more so at the higher flight Mach number. Not only are the magnitudes of the effects greater, but also the effects of compressor pressure ratio are more pronounced with the nonafterburning engine. The decrease in relative thrust and increase in relative thrust specific fuel consumption are almost linear with shaft power extraction.

As an example of possible effects on engine performance due to shaft power extraction for operating a refrigerating system, consider the power parameters of 0.80 and 0.30 for the air and mercury-vapor cycles, respectively, that were used in a previous illustration for $\varepsilon_h = \varepsilon_e = 0.8$ and $\varepsilon_c \frac{(wc_p)_R}{(wc_p)_a} = 4$. Also assume that 5 percent of the compressor air is bled off for refrigeration (a reasonable value for turbine cooling purposes) and that the bleed temperature T_1 is 1500° R. The shaft power extraction parameter can be calculated from

$$\frac{\mathscr{P}_t}{w_E} = \frac{\mathscr{P}_t}{w_a c_{p,a} T_1} \left(\frac{w_a}{w_E}\right)\left(c_{p,a} T_1\right) \tag{15}$$

The following table lists the relative thrusts and thrust specific fuel consumptions obtained from figure 13 for an engine with a compressor pressure ratio of 4 at a flight Mach number of 2.5:

Engine	Air cycle			Mercury-vapor cycle		
	$\mathscr{P}_t/w_E$	Relative thrust	Relative thrust specific fuel consumption	$\mathscr{P}_t/w_E$	Relative thrust	Relative thrust specific fuel consumption
Nonafterburning	14.95	0.927	1.078	5.60	0.974	1.026
Afterburning	14.95	.972	1.050	5.60	.991	1.017

[redacted]

From the preceding table, which considers only the performance losses due to engine shaft power extraction, it can be seen that the power extraction required for the air cycle can cause the thrust to be reduced over 7 percent and the thrust specific fuel consumption increased by about the same percentage. For the mercury-vapor cycle the performance losses from power extraction are about one-third as great. If an aftercooler will serve satisfactorily so that an air or vapor cycle is not required, there will be practically no power extraction. For both air and mercury-vapor cycles, the afterburning engine has a smaller loss in thrust than the nonafterburning engine because exhaust-gas temperature is maintained constant by burning more fuel in the afterburner. The loss in thrust for the afterburning engine is entirely due to a lower pressure in the exhaust nozzle caused by a larger required pressure drop across the turbine. For the nonafterburning engine the thrust is decreased by a reduction in both temperature and pressure of the exhaust gases.

The performance losses listed in the table do not include the effects of bleeding air from the compressor or the effects of pressure losses or heat addition if engine air is the receiving fluid. The effects of bleeding air from the compressor are discussed in reference 11. Such effects may be greater than the losses due to power extraction of the mercury-vapor refrigeration cycle, but will probably be less than the power extraction losses for the air cycle. By refrigerating the cooling air, the quantity that must be bled for turbine cooling can be reduced. It is possible that in some cases there may be a net gain in performance using refrigeration because of the smaller quantity of air required for cooling.

Each application of any of these systems to an engine will be a unique case. A performance study will have to be made to determine effects of quantity of bleed air required, power extraction, and system weight on engine performance for a wide variety of systems to pick the system that will result in the best over-all engine performance. The study included herein cannot be generalized to the point of determining which will be the best system for every application, but use of the generalized curves that are presented will permit the engine designer to analyze the effects of these systems on his particular engine.

CONCLUSIONS

The conclusions drawn from a thermodynamic study of air-cycle and mercury-vapor-cycle refrigeration devices can be summarized as follows:

1. For compressor and turbine efficiencies (about 0.70) that seem feasible for small units, a heat-exchanger effectiveness of almost 0.8 is required before an air cycle can be used to obtain a greater air temperature reduction than is possible with an aftercooler with the same heat-exchanger effectiveness. At these conditions, however, the air cycle can also be used as a heat pump (receiver temperature higher than air-cycle inlet temperature).

[redacted]

2. A convenient method for absorbing the power developed by the auxiliary (expansion) turbine in an air cycle is to couple it to an auxiliary compressor. The allowable pressure ratio permitted by this power source is so low, however, that it will not contribute to an appreciable reduction in the air-cycle outlet temperature.

3. A system employing a mercury-vapor cycle appears to be feasible for refrigerating air that must enter the system at temperature levels of approximately 1500° R, and this cycle is more efficient than the air cycle. Weight was not considered in evaluating these two systems; such a study would be required before a final choice of a system could be made.

5014

4. It appears that the power required for the mercury-vapor cycle may have a smaller effect on engine performance than bleeding air from the compressor. By refrigerating the cooling air to reduce the quantity required, there may possibly be a net gain in engine performance in some cases.

Lewis Flight Propulsion Laboratory
National Advisory Committee for Aeronautics
Cleveland, Ohio, July 18, 1956

[redacted]

APPENDIX A

SYMBOLS

c_p specific heat at constant pressure, Btu/(lb)($^\circ$R)

$\mathscr{E}$ heat-exchanger effectiveness by basic definition (eqs. (6), (13), or (14))

H refrigerant enthalpy, Btu/lb

M flight Mach number

m slope of line as defined in eq. (C13)

P stagnation pressure, lb/sq ft

$\mathscr{P}$ power, Btu/sec

Q total heat-transfer rate, Btu/sec

S refrigerant entropy, Btu/(lb)($^\circ$R)

T stagnation temperature, $^\circ$R

w weight flow, lb/sec

γ ratio of specific heats

η component adiabatic efficiency

η^* fictitious auxiliary-turbine efficiency defined by eq. (2)

ψ heat-exchanger pressure-drop parameter

ε heat-exchanger effectiveness for $\frac{(wc_p)_a}{(wc_p)_{min}}$ or $\frac{(wc_p)_R}{(wc_p)_{min}} = 1.0$ (eqs. (5), (C11), or (C12))

Subscripts:

a air

C compressor (stations 1 to 3 for air cycle; stations x to y for mercury-vapor cycle)

[redacted]

c	condenser in mercury-vapor cycle, or mercury vapor in condenser
E	engine air
e	evaporator in mercury-vapor cycle, or mercury vapor in evaporator
h	heat exchanger in air cycle
id	ideal
l	liquid refrigerant
min	minimum
R	receiver
r	refrigerant (when used with w refers to total refrigerant weight flow)
T	auxiliary turbine
t	total
v	vapor refrigerant
w,x, y,z	stations in mercury-vapor compression cycle (fig. 5)
1,2,3, 4,5	stations in air-cycle refrigeration system (fig. 1)

APPENDIX B

DERIVATION OF WORKING EQUATIONS FOR AIR-CYCLE REFRIGERATION

For the air-cycle refrigeration system it is specified that the pressures out of and into the system (fig. 1) are equal, that is, $P_5 = P_1$. Thus, $P_1 = P_5$ is the pressure at which air could be bled interstage from the engine compressor and supplied to the turbine for cooling. If the associated bleed temperature T_1 is not low enough for cooling purposes, a lower temperature T_5 can be obtained by employing the system illustrated in figure 1. However, energy external to the cycle must be expended to operate the system. This expenditure of energy is necessary because of the component inefficiencies and pressure drop in the heat exchanger. Since the engine compressor is usually more efficient than the smaller auxiliary compressor, the air is not bled from the compressor until after it is compressed to engine compressor-discharge pressure. Thus, the energy expended on the bleed air in the main engine compressor is

$$\mathscr{P}_{1-2} = w_a c_{p,a}(T_2 - T_1) \tag{B1}$$

The bleed air can then be further compressed in an auxiliary compressor. After cooling, the bleed air in the heat exchanger can be expanded through the auxiliary turbine to further reduce its temperature and also to recover some of the energy expended in the compressors. The net energy expenditure to the auxiliary-compressor and -turbine combination is

$$\mathscr{P}_{2-5} = w_a c_{p,a}(T_3 - T_2) - w_a c_{p,a}(T_4 - T_5) \tag{B2}$$

Obviously the total energy to operate the system is

$$\mathscr{P}_t = \mathscr{P}_{1-2} + \mathscr{P}_{2-5} = w_a c_{p,a}(T_3 - T_1) - w_a c_{p,a}(T_4 - T_5) \tag{B3}$$

This can also be expressed as

$$\mathscr{P}_t = \frac{w_a c_{p,a} T_1}{\eta_{C,a}}\left[\left(\frac{P_3}{P_1}\right)^{\frac{\gamma-1}{\gamma}} - 1\right] - w_a c_{p,a}\eta^* T_5\left[\left(\frac{P_4}{P_5}\right)^{\frac{\gamma-1}{\gamma}} - 1\right] \tag{B4}$$

where η^* is a fictitious turbine efficiency and $\eta_{C,a}$ is the efficiency of the entire cycle compressor process from stations 1 to 3. The relation between η^* and η_T based on turbine-inlet temperature can be obtained as follows. Using η_T to express auxiliary-turbine work,

$$w_a c_{p,a}(T_4 - T_5) = w_a c_{p,a}\eta_T T_4 \left[1 - \left(\frac{P_5}{P_4}\right)^{\frac{\gamma-1}{\gamma}}\right] \tag{B5}$$

Using η^* to express turbine work,

$$w_a c_{p,a}(T_4 - T_5) = w_a c_{p,a}\eta^* T_5 \left[\left(\frac{P_4}{P_5}\right)^{\frac{\gamma-1}{\gamma}} - 1\right] \tag{B6}$$

From equation (B5)

$$\frac{T_5}{T_4} = 1 - \eta_T\left[1 - \left(\frac{P_5}{P_4}\right)^{\frac{\gamma-1}{\gamma}}\right] \tag{B5a}$$

Dividing equation (B6) by T_4, solving for η^*, and substituting equation (B5a) for T_5/T_4 yield

$$\eta^* \equiv \frac{\eta_T\left[1 - \left(\frac{P_5}{P_4}\right)^{\frac{\gamma-1}{\gamma}}\right]}{\left\{1 - \eta_T\left[1 - \left(\frac{P_5}{P_4}\right)^{\frac{\gamma-1}{\gamma}}\right]\right\}\left[\left(\frac{P_4}{P_5}\right)^{\frac{\gamma-1}{\gamma}} - 1\right]} \tag{2}$$

Since $P_1 = P_5$, $\frac{P_4}{P_5} = \frac{P_3}{P_1}\frac{P_4}{P_3}$. Dividing equation (B4) by $w_a c_{p,a} T_1$ and defining

$$\Psi \equiv \frac{\left(\frac{P_3}{P_1}\frac{P_4}{P_3}\right)^{\frac{\gamma-1}{\gamma}} - 1}{\left(\frac{P_3}{P_1}\right)^{\frac{\gamma-1}{\gamma}} - 1} \tag{3}$$

yield

$$\eta_{C,a}\eta^{*}\psi \frac{T_5}{T_1} = 1 - \frac{\eta_{C,a}\left(\frac{\mathscr{P}_t}{w_a c_{p,a} T_1}\right)}{\left[\left(\frac{P_3}{P_1}\right)^{\frac{\gamma-1}{\gamma}} - 1\right]} \tag{1}$$

which is a general expression relating the work and temperature ratio for the air cycle.

When the product wc_p for bleed air is the smaller of the two fluids used in a heat exchanger, the heat-exchanger effectiveness can be expressed as follows:

$$\varepsilon_h = \frac{T_3 - T_4}{T_3 - T_R} \tag{5}$$

From an energy balance of the system,

$$T_3 - T_4 = T_1 - T_5 + \frac{\mathscr{P}_t}{w_a c_{p,a}} \tag{B7}$$

Substituting equation (B7) into equation (5) and dividing by T_1 yield

$$\varepsilon_h = \frac{1 - \frac{T_5}{T_1} + \frac{\mathscr{P}_t}{w_a c_{p,a} T_1}}{\frac{T_3}{T_1} - \frac{T_R}{T_1}} \tag{B8}$$

The compression temperature ratio is

$$\frac{T_3}{T_1} = 1 + \frac{1}{\eta_{C,a}}\left[\left(\frac{P_3}{P_1}\right)^{\frac{\gamma-1}{\gamma}} - 1\right] \tag{B9}$$

Substituting equation (B9) into equation (B8) yields

$$\varepsilon_h = \frac{1 - \frac{T_5}{T_1} + \frac{\mathscr{P}_t}{w_a c_{p,a} T_1}}{1 + \frac{1}{\eta_{C,a}}\left[\left(\frac{P_3}{P_1}\right)^{\frac{\gamma-1}{\gamma}} - 1\right] - \frac{T_R}{T_1}} \tag{B10}$$

Solving for $\mathscr{P}_t/w_a c_{p,a} T_1$ from equation (B10), substituting it into equation (1), and solving for T_5/T_1 yield

$$\frac{T_5}{T_1} = \frac{\left\{ \frac{1}{\eta_{C,a}} \left[\left(\frac{P_3}{P_1} \right)^{\frac{\gamma-1}{\gamma}} - 1 \right] + 1 \right\} (1 - \varepsilon_h) + \varepsilon_h \frac{T_R}{T_1}}{\eta^* \psi \left[\left(\frac{P_3}{P_1} \right)^{\frac{\gamma-1}{\gamma}} - 1 \right] + 1} \tag{4}$$

which relates the air-cycle temperature ratio T_5/T_1 to the heat-exchanger effectiveness ε_h and the temperature ratio T_R/T_1.

When no external power is supplied to the shaft of the auxiliary compressor and turbine ($\mathscr{P}_{2-5} = 0$), equation (B2) combined with equation (B6) becomes

$$\frac{T_2}{\eta_{C,a}} \left[\left(\frac{P_3}{P_2} \right)^{\frac{\gamma-1}{\gamma}} - 1 \right] = \eta^* T_5 \left[\left(\frac{P_4}{P_5} \right)^{\frac{\gamma-1}{\gamma}} - 1 \right] \tag{B11}$$

Substituting equation (3) in equation (B11) and dividing by T_1 yield

$$\frac{T_2}{\eta_{C,a} T_1} \left[\left(\frac{P_3}{P_2} \right)^{\frac{\gamma-1}{\gamma}} - 1 \right] = \eta^* \psi \frac{T_5}{T_1} \left[\left(\frac{P_3}{P_1} \right)^{\frac{\gamma-1}{\gamma}} - 1 \right] \tag{B12}$$

Since $\mathscr{P}_{2-5} = 0$, equation (B3) becomes

$$\mathscr{P}_t = w_a c_{p,a} (T_2 - T_1) \tag{B13}$$

Dividing equation (B13) by $w_a c_{p,a} T_1$ and transposing yield

$$\frac{T_2}{T_1} = 1 + \frac{\mathscr{P}_t}{w_a c_{p,a} T_1} \tag{B14}$$

5014

[redacted]

Substituting equation (B14) into equation (B12) yields the following expression for the auxiliary-compressor pressure ratio:

$$\frac{P_3}{P_2} = \left\{ 1 + \frac{\eta_{C,a}\eta^*\psi \frac{T_5}{T_1}\left[\left(\frac{P_3}{P_1}\right)^{\frac{\gamma-1}{\gamma}} - 1\right]}{1 + \frac{\mathscr{P}_t}{w_a c_{p,a} T_1}} \right\}^{\frac{\gamma}{\gamma-1}} \tag{7}$$

APPENDIX C

DERIVATION OF WORKING EQUATIONS FOR SYSTEM WITH MERCURY-VAPOR COMPRESSION CYCLE

The mercury-vapor cycle is illustrated schematically in figure 5. It can be seen that on the air side the heat exchanger between stations 3 and 4 has been replaced by the evaporator of the mercury-vapor compression cycle and that the auxiliary compressor and turbine are not present. Thus, in order to retain stations 1 and 5 as inlet and outlet, respectively, for the air side of the system, $P_4/P_5 = 1$, $T_4/T_5 = 1$, $P_3/P_2 = 1$, and $T_3/T_2 = 1$. The air temperature-reduction ratio across the evaporator T_4/T_3 can be related to the rate of heat removal from the air by the following equation:

$$Q_{3-4} = w_a c_{p,a}(T_3 - T_4) = w_a c_{p,a} T_3 \left(1 - \frac{T_4}{T_3}\right) \qquad (C1)$$

The power required to achieve this heat flow rate against an adverse temperature-difference can be determined from a thermodynamic analysis of the mercury-vapor compression cycle. The thermodynamic cycle of the mercury refrigerant is illustrated in figure 6. Station w represents a mixture of liquid and vapor refrigerant at the inlet to the evaporator. As the refrigerant flows through the evaporator, the liquid portion absorbs the heat rejected by the bleed air. This heat absorption is accomplished by evaporation of a portion of the liquid refrigerant at a constant pressure and temperature. The mixture of liquid and vapor refrigerant at station x (with a higher concentration of vapor than entered the evaporator) is then compressed to the saturated vapor line at station y. As seen from figure 6, the efficiency of compression determines the work ΔH required to achieve a saturated vapor. The temperature associated with the saturation pressure at station y is sufficiently higher than that of the heat receiver in the condenser so that the heat absorbed in the evaporator plus the work of compression can be rejected. Heat rejection in the condenser takes place at constant pressure and temperature with change in state from saturated vapor at station y to saturated liquid at station z. In order for the saturated liquid to be returned to the evaporator in a state capable of absorbing more heat, the refrigerant is expanded through a throttling valve to the saturation temperature and pressure in the evaporator (station w). Since throttling is a constant enthalpy process, it is necessary for a portion of the liquid to flash to vapor during the process. This accounts for the mixture of liquid and vapor entering the evaporator at station w.

In this study, it was desirable to know how the work necessary to operate the cycle varied with the rate of moving heat and the temperature difference against which it is moved.

For isentropic compression the following two equations apply:

$$w_r H_{v,y} - w_{l,x} H_{l,x} - (w_r - w_{l,x}) H_{v,x} = w_r \Delta H_{C,id} \tag{C2}$$

$$w_{l,x} S_{l,x} + (w_r - w_{l,x}) S_{v,x} = w_r S_{v,y} \tag{C3}$$

Dividing equations (C2) and (C3) by w_r gives

$$\Delta H_{C,r,id} = \frac{w_{l,x}}{w_r} (H_{v,x} - H_{l,x}) + H_{v,y} - H_{v,x} \tag{C2a}$$

$$\frac{w_{l,x}}{w_r} = \frac{S_{v,y} - S_{v,x}}{S_{l,x} - S_{v,x}} \tag{C3a}$$

Substituting equation (C3a) into equation (C2a) and dividing by the compressor efficiency yield the actual work per pound of refrigerant to operate the system:

$$\Delta H_{C,r} = \left[\frac{(S_{v,y} - S_{v,x})(H_{v,x} - H_{l,x})}{(S_{l,x} - S_{v,x}) \eta_{C,r}} \right] + \frac{H_{v,y} - H_{v,x}}{\eta_{C,r}} \tag{C4}$$

The condensing process from station y to z can be expressed by the following equation:

$$Q + w_r \Delta H_{C,r} = w_r (H_{v,y} - H_{l,z}) \tag{C5}$$

Solving equation (C5) for w_r yields

$$w_r = \frac{Q}{H_{v,y} - H_{l,z} - \Delta H_{C,r}} \tag{C5a}$$

Since $w_r \Delta H_{C,r}$ is the power to operate the mercury-vapor compression cycle, let $w_r \Delta H_{C,r} = \mathscr{P}_r$. Combining equations (C4) and (C5a) gives

$$\mathscr{P}_r = \frac{Q}{\left[\frac{(H_{v,y} - H_{l,z}) \eta_{C,r}}{\frac{(S_{v,y} - S_{v,x})(H_{v,x} - H_{l,x})}{S_{l,x} - S_{v,x}} + H_{v,y} - H_{v,x}} \right] - 1} \tag{C6}$$

[redacted]

Equation (C6) can be made dimensionless; thus,

$$\frac{\mathscr{P}_r}{Q} = \frac{1}{\left[\frac{(H_{v,y} - H_{l,z})\eta_{C,r}}{\frac{(S_{v,y} - S_{v,x})(H_{v,x} - H_{l,x})}{S_{l,x} - S_{v,x}} + H_{v,y} - H_{v,x}}\right] - 1} \tag{C7}$$

Substituting equation (C1) into equation (C6) and transposing yield

$$\frac{T_4}{T_3} = 1 - \frac{\mathscr{P}_r}{w_a c_{p,a} T_3}\left\{\left[\frac{\eta_{C,r}(H_{v,y} - H_{l,z})}{\frac{(S_{v,y} - S_{v,x})(H_{v,x} - H_{l,x})}{S_{l,x} - S_{v,x}} + H_{v,y} - H_{v,x}}\right] - 1\right\} \tag{9}$$

In order to compare the mercury-vapor compression cycle on the same basis as the air cycle, the energy expended to overcome the air pressure drop in the evaporator must be taken into account since it is specified that $P_5 = P_1$. This requires that prior to refrigeration in the evaporator the air pass through a compressor with a pressure ratio sufficient to overcome the evaporator pressure drop:

$$\frac{P_2}{P_1} = \frac{P_3}{P_1} = \frac{1}{P_4/P_3} \tag{C8}$$

The energy required for this compression is

$$\frac{\mathscr{P}_{1\text{-}3}}{w_a c_{p,a}} = T_3 - T_1 = \frac{T_1}{\eta_{C,a}}\left[\left(\frac{P_3}{P_1}\right)^{\frac{\gamma-1}{\gamma}} - 1\right] \tag{C9}$$

Substituting equation (C8) into equation (C9) and dividing by T_1 yield

$$\frac{\mathscr{P}_{1\text{-}3}}{w_a c_{p,a} T_1} = \frac{T_3}{T_1} - 1 = \frac{1}{\eta_{C,a}}\left[\left(\frac{1}{P_4/P_3}\right)^{\frac{\gamma-1}{\gamma}} - 1\right] \tag{C10}$$

From the equality on the right,

$$\frac{T_3}{T_1} = 1 + \frac{1}{\eta_{C,a}}\left[\left(\frac{1}{P_4/P_3}\right)^{\frac{\gamma-1}{\gamma}} - 1\right] \tag{C10a}$$

Therefore, since $T_5/T_4 = 1$,

$$\frac{T_5}{T_1} = \frac{T_4}{T_3}\left\{1 + \frac{1}{\eta_{C,a}}\left[\left(\frac{1}{P_4/P_3}\right)^{\frac{\gamma-1}{\gamma}} - 1\right]\right\} \tag{11}$$

which expresses the temperature ratio for the entire system. The total energy expended in this system is the sum of that shown in equations (9) and (C10):

$$\frac{\mathscr{P}_t}{w_a c_{p,a} T_1} = \frac{\mathscr{P}_r}{w_a c_{p,a} T_3}\left(\frac{T_3}{T_1}\right) + \frac{T_3}{T_1} - 1$$

Factoring T_3/T_1 and substituting for it from equation (C10a) yield

$$\frac{\mathscr{P}_t}{w_a c_{p,a} T_1} = \left(\frac{\mathscr{P}_r}{w_a c_{p,a} T_3} + 1\right)\left\{1 + \frac{1}{\eta_{C,a}}\left[\left(\frac{1}{P_4/P_3}\right)^{\frac{\gamma-1}{\gamma}} - 1\right]\right\} - 1 \tag{10}$$

The obtainable air temperature-reduction ratio across the evaporator can also be expressed in terms of the evaporator effectiveness and evaporation temperature by means of equation (5) with revision of subscripts:

$$\varepsilon_e = \frac{T_3 - T_4}{T_3 - T_e} \tag{C11}$$

The condenser effectiveness can be expressed as

$$\varepsilon_c = \frac{\frac{(wc_p)_a}{(wc_p)_R}\left[(T_3 - T_4) + \frac{\mathscr{P}_r}{(wc_p)_a}\right]}{T_c - T_R} \tag{C12}$$

There is a linear relation between $\mathscr{P}_r/w_a c_{p,a} T_3$ and T_4/T_3 in equation (9) (see fig. 11) if the temperature ratio T_c/T_e is maintained constant. From numerical values obtained from equation (9), the following expression may be written:

$$\frac{\mathscr{P}_r}{w_a c_{p,a} T_3} = \left(\frac{T_4}{T_3} - 1\right)\frac{1}{m} \tag{C13}$$

where values of $1/m$ for the mercury-vapor cycle are as follows:

T_c/T_e	$1/m$
1.1	-0.240
1.2	-.540
1.3	-.945
1.4	-1.53
1.5	-3.01

Combining equations (C11) to (C13) results in

$$\frac{T_4}{T_3} = \frac{\varepsilon_c \frac{(wc_p)_R}{(wc_p)_a}\left(\frac{1}{\varepsilon_e}\frac{T_c}{T_e} + \frac{T_R}{T_3} - \frac{T_c}{T_E}\right) + 1 - \frac{1}{m}}{\varepsilon_c \frac{(wc_p)_R}{(wc_p)_a}\frac{1}{\varepsilon_e}\frac{T_c}{T_e} + 1 - \frac{1}{m}} \tag{12}$$

5014

REFERENCES

1. Mason, J. L., Burriss, W. L., and Connolly, T. J.: Vapor-Cycle Cooling for Aircraft. WADC Tech. Rep. 53-338, Wright Air Dev. Center, Air Res. and Dev. Command, Wright-Patterson Air Force Base, Oct. 1953. (Contract AF 33(616)-2016.)

2. Burgess, G. A.: Design Analysis of Several Cabin Cooling Systems for Jet-Propelled Aircraft. Rep. No. AAC-290-R, AiResearch Mfg. Co., Los Angeles (Calif.), Nov. 1947.

3. Stevens, L. R., Jr.: A Systematic Study of Air Cycles for Aircraft Cooling Applications. Paper No. 56-SA-11, A.S.M.E., 1956.

4. Schramm, Wilson B., Nachtigall, Alfred J., and Arne, Vernon L.: Analytical Comparison of Turbine-Blade Cooling Systems Designed for a Turbojet Engine Operating at Supersonic Speed and Altitude. I - Liquid-Cooling Systems. NACA RM E52J29, 1953.

5. Schramm, Wilson B., Arne, Vernon L., and Nachtigall, Alfred J.: Analytical Comparison of Turbine-Blade Cooling System Designed for a Turbojet Engine Operating at Supersonic Speed and Altitude. II - Air-Cooling Systems. NACA RM E52J30, 1953.

6. Eckert, E. R. G., and Diaguila, Anthony J.: Method of Calculating Core Dimensions of Crossflow Heat Exchanger with Prescribed Gas Flows and Inlet and Exit States. NACA TN 3655, 1956.

7. Diaguila, Anthony J., Livingood, John N. B., and Eckert, Ernst R. G.: Study of Ram-Air Heat Exchangers for Reducing Turbine Cooling-Air Temperature of a Supersonic Aircraft Turbojet Engine. NACA RM E56E17, 1956.

8. Esgar, Jack B., and Slone, Henry O.: Gas-Turbine-Engine Performance When Heat from Liquid-Cooled Turbines is Rejected Ahead of, Within, or Behind the Compressor. NACA RM E56B09, 1956.

9. Van Winkle, J.: A Survey of Possible Refrigerants for High-Temperature Application. Paper No. 56-SA-12, A.S.M.E., 1956.

10. Sheldon, Lucian A.: Thermodynamic Properties of Mercury Vapor. Paper No. 49-A-30, A.S.M.E., 1950.

11. Esgar, Jack B., and Ziemer, Robert R.: Effect of Turbine Cooling with Compressor Air Bleed on Gas-Turbine Engine Performance. NACA RM E54L20, 1955.

12. Esgar, Jack B., and Ziemer, Robert R.: Methods for Rapid Graphical Evaluation of Cooled or Uncooled Turbojet and Turboprop Engine or Component Performance (Effects of Variable Specific Heat Included). NACA TN 3335, 1955.

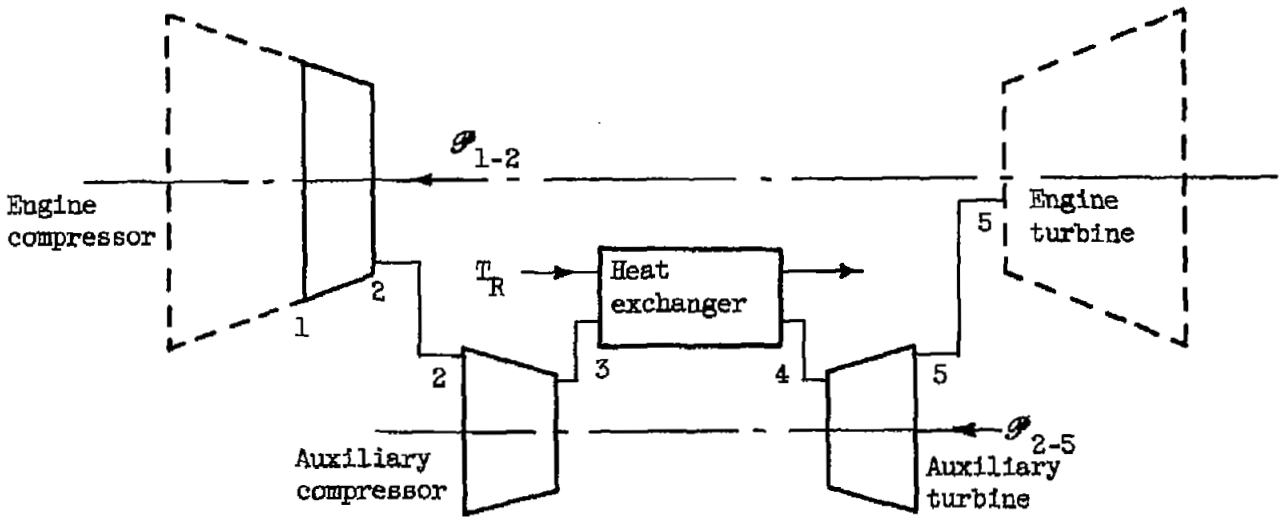

Figure 1. - Air-cycle refrigeration system.

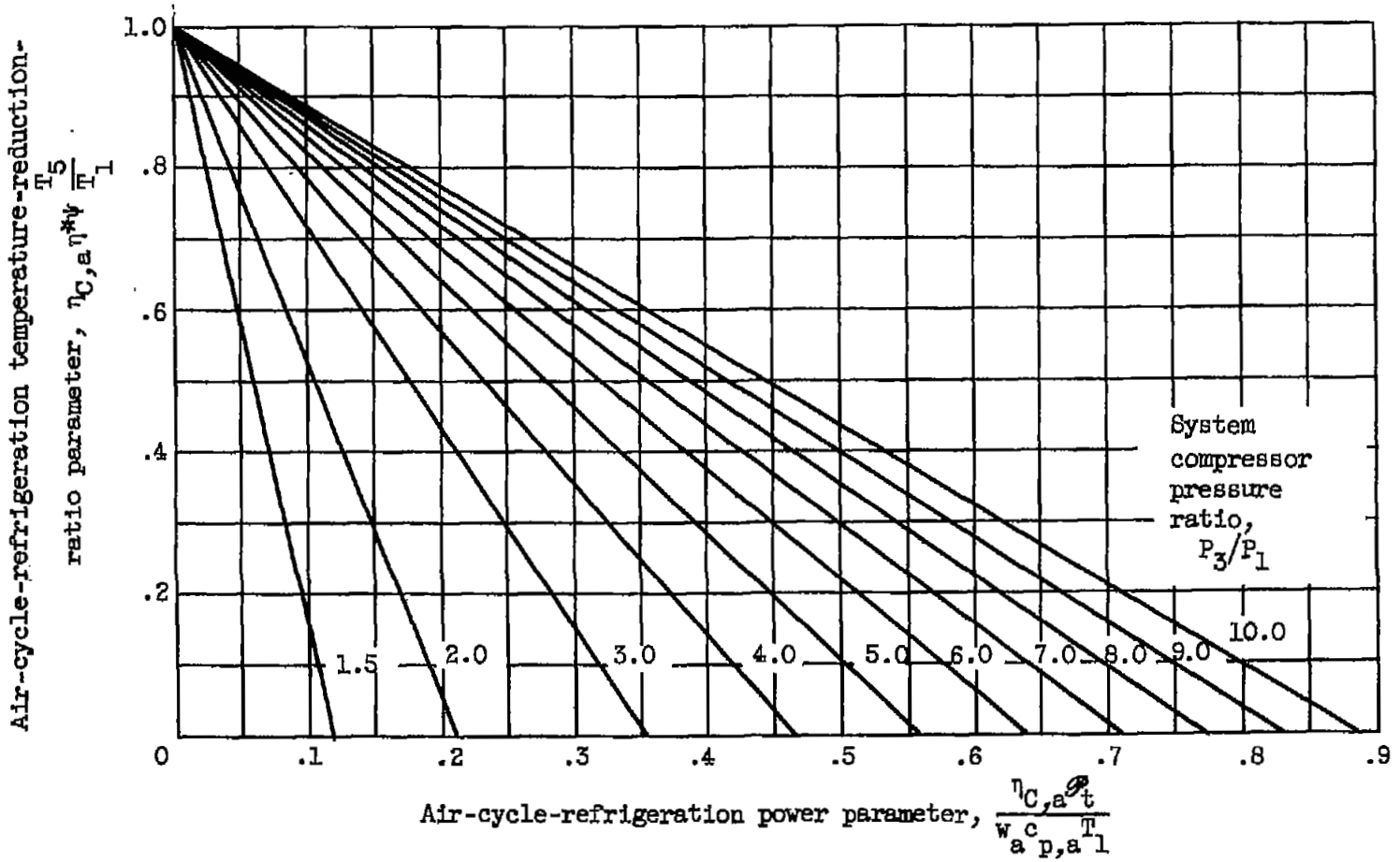

Figure 2. - Variation of air temperature-reduction parameter with refrigeration power parameter over range of air-cycle-system compressor pressure ratios.

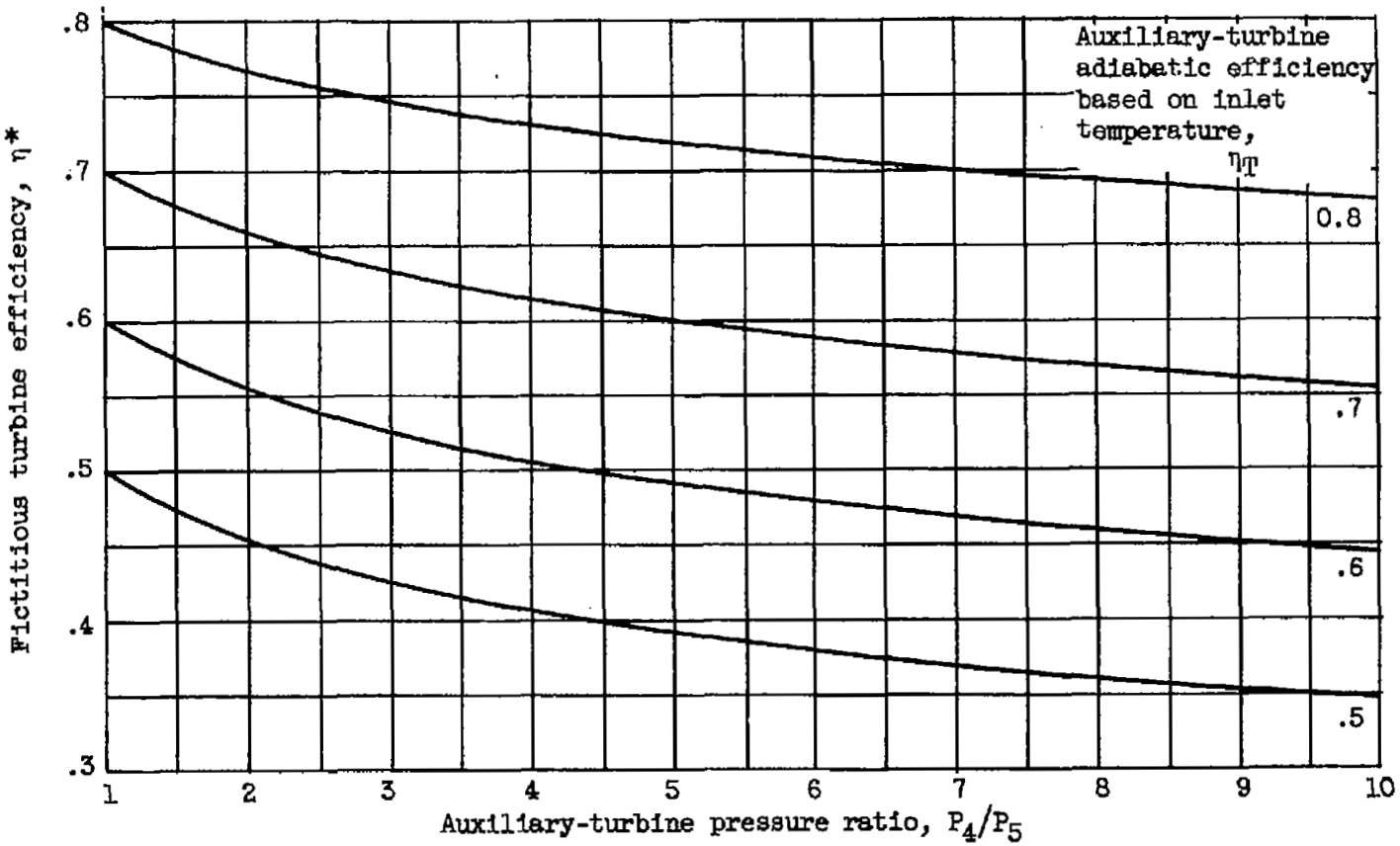

Figure 3. - Variation of fictitious turbine efficiency with turbine pressure ratio for various values of auxiliary-turbine adiabatic efficiency.

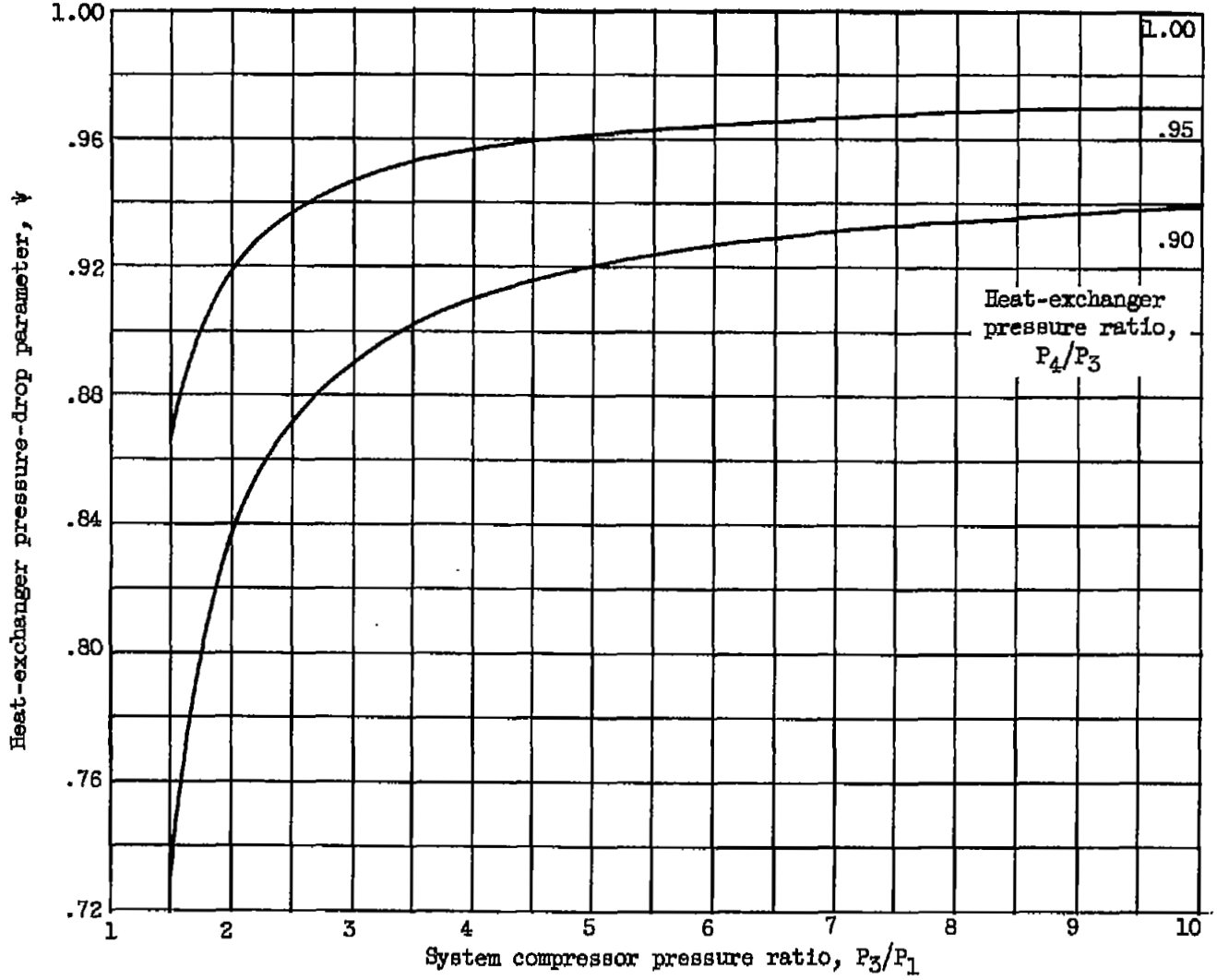

Figure 4. - Variation of heat-exchanger pressure-drop parameter with air-cycle-system compressor pressure ratio.

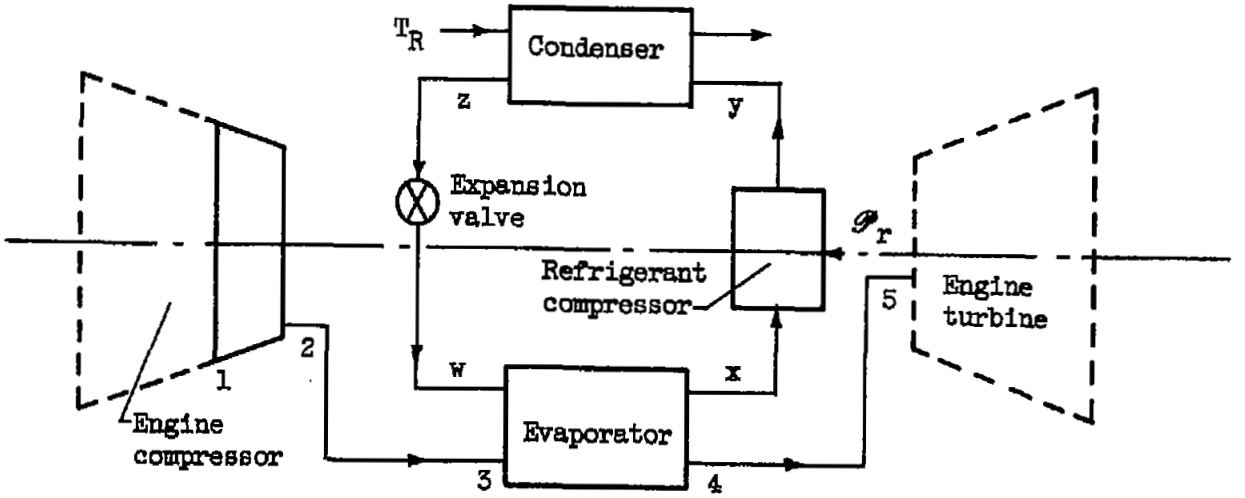

Figure 5. - Mercury-vapor-cycle refrigeration system.

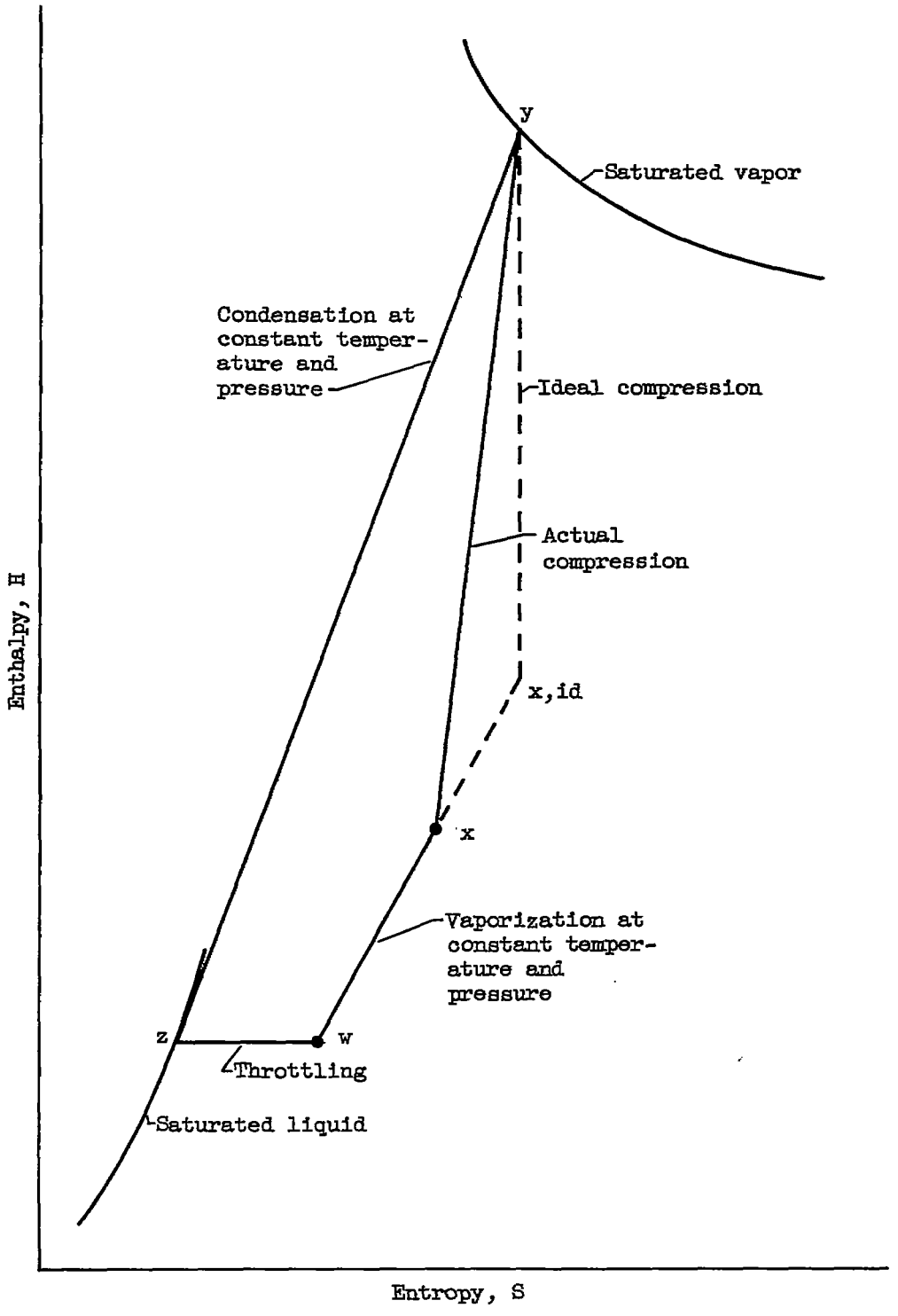

Figure 6. - Enthalpy-entropy diagram for mercury-vapor cycle.

[redacted]

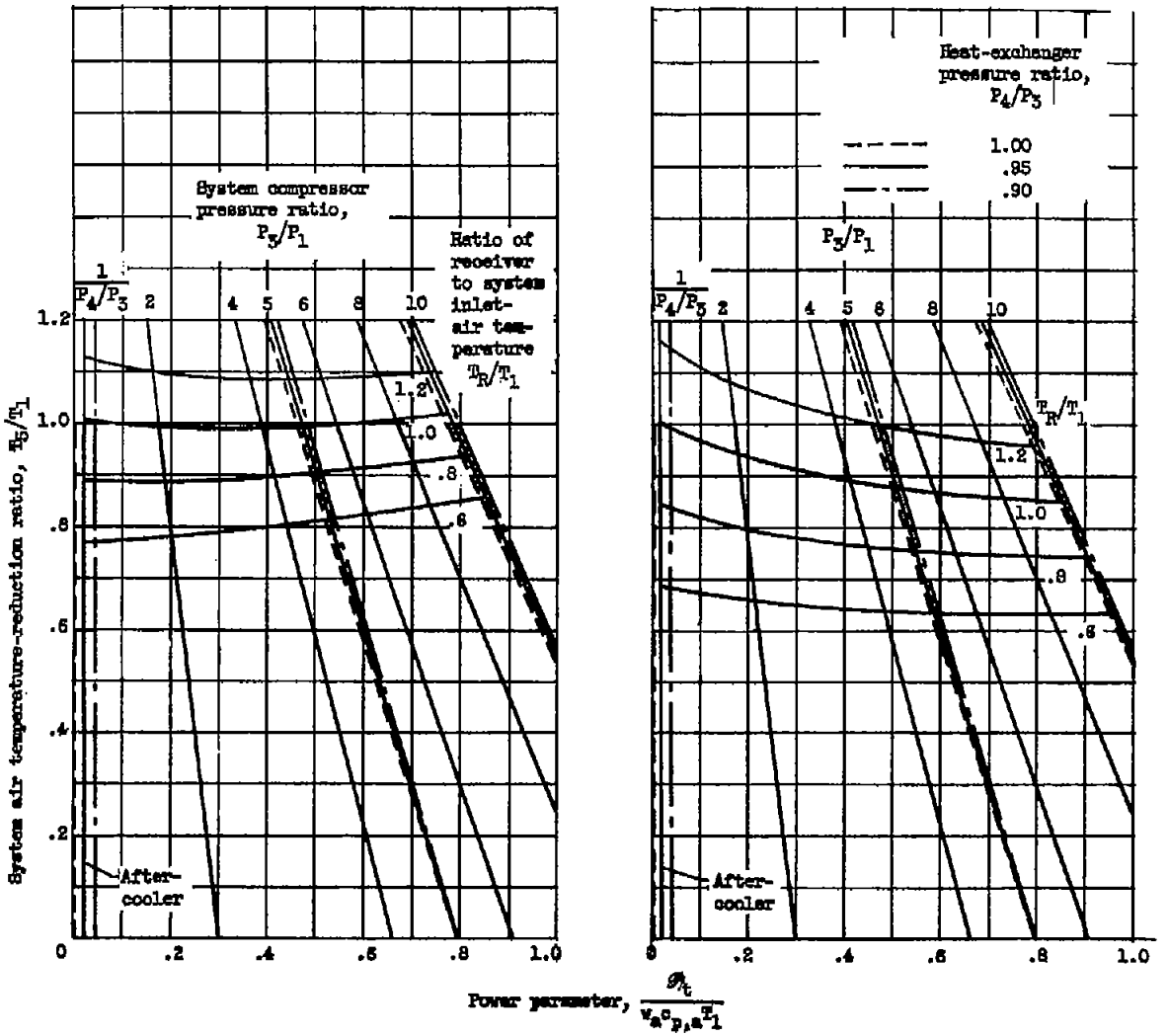

(a) Heat-exchanger effectiveness, 0.6.

(b) Heat-exchanger effectiveness, 0.8.

Figure 7. - Performance plot for air-cycle refrigeration system. System compressor and turbine adiabatic efficiencies, 0.70.

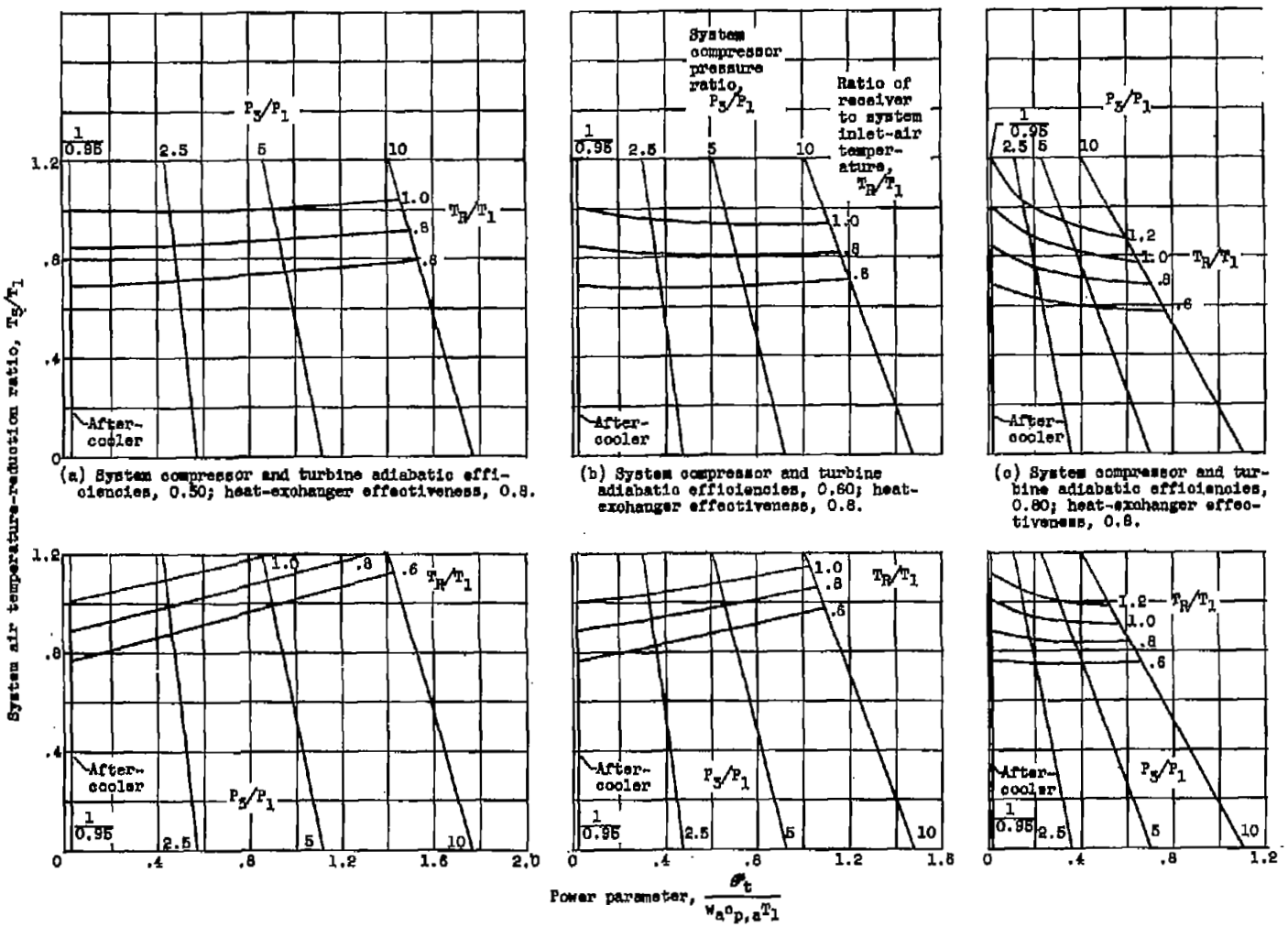

(a) System compressor and turbine adiabatic efficiencies, 0.50; heat-exchanger effectiveness, 0.8.

(b) System compressor and turbine adiabatic efficiencies, 0.60; heat-exchanger effectiveness, 0.8.

(c) System compressor and turbine adiabatic efficiencies, 0.80; heat-exchanger effectiveness, 0.8.

(d) System compressor and turbine adiabatic efficiencies, 0.80; heat-exchanger effectiveness, 0.6.

(e) System compressor and turbine adiabatic efficiencies, 0.60; heat-exchanger effectiveness, 0.6.

(f) System compressor and turbine adiabatic efficiencies, 0.80; heat-exchanger effectiveness, 0.6.

Figure 8. - Effect of system component efficiencies on performance of air-cycle refrigeration system for two values of heat-exchanger effectiveness. Heat-exchanger pressure ratio, 0.95.

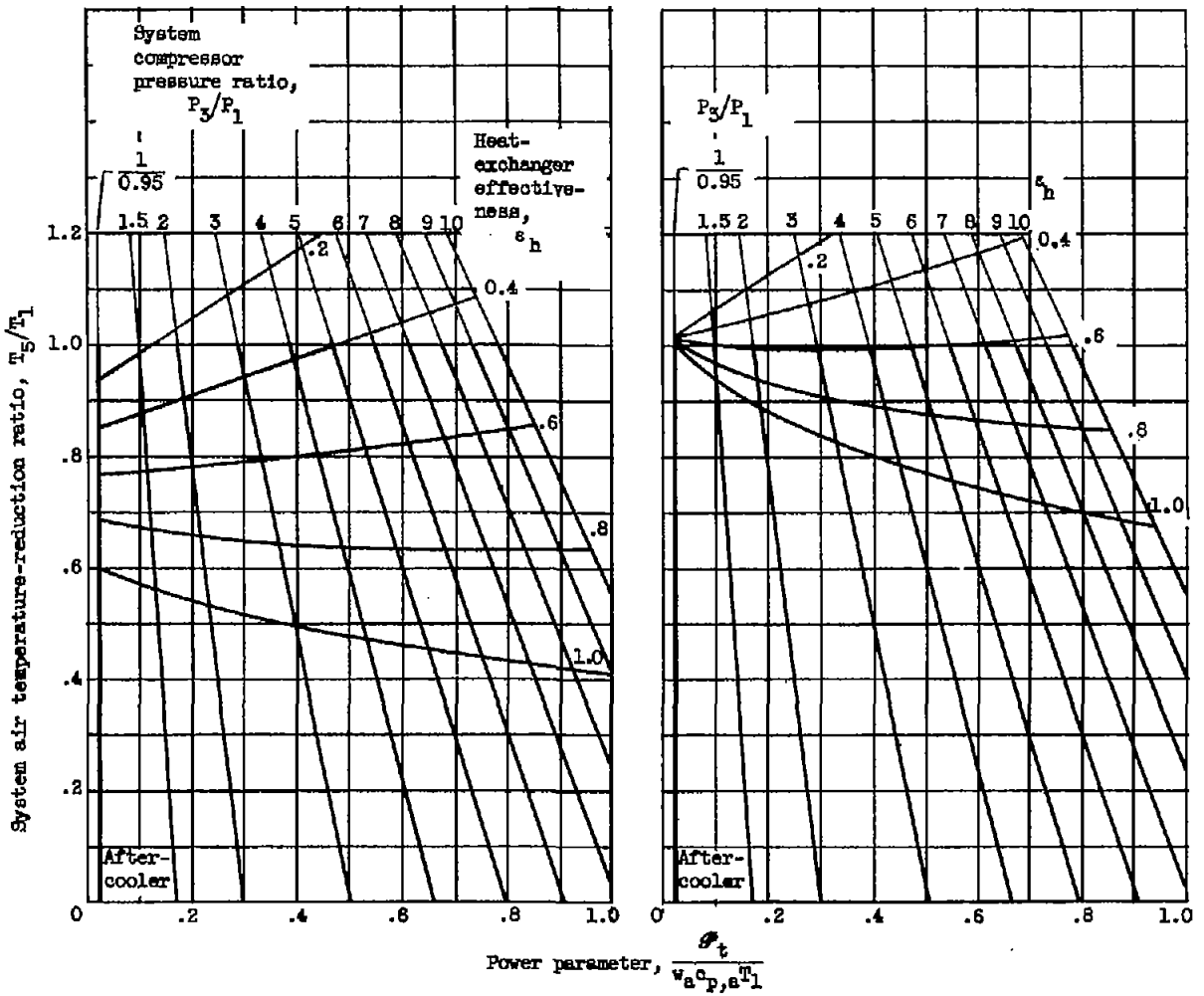

(a) Ratio of receiver to system inlet-air temperature, 0.6.

(b) Ratio of receiver to system inlet-air temperature, 1.0.

Figure 9. - Effect of heat-exchanger effectiveness on performance of air-cycle refrigeration system. System compressor and turbine adiabatic efficiencies, 0.70; heat-exchanger pressure ratio, 0.95.

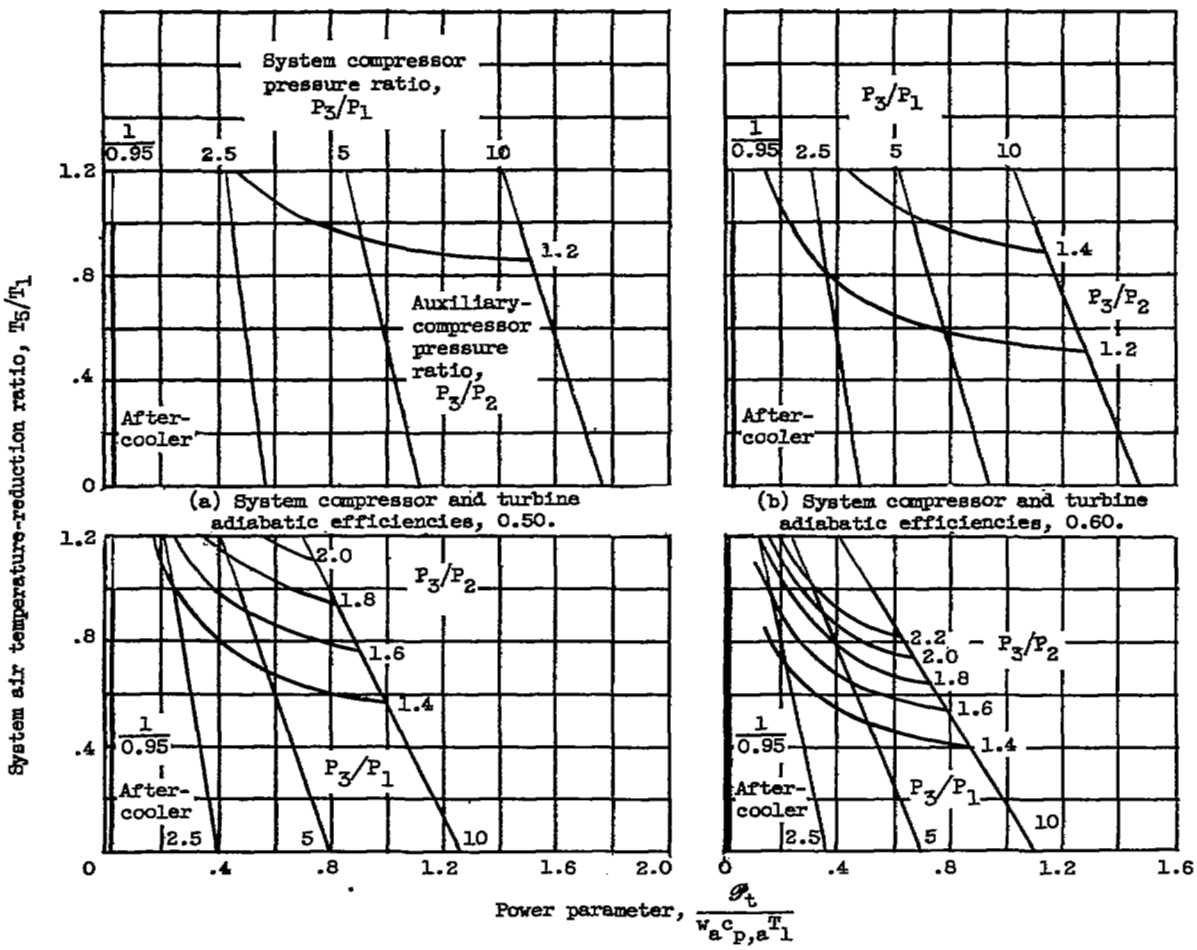

(a) System compressor and turbine adiabatic efficiencies, 0.50.

(b) System compressor and turbine adiabatic efficiencies, 0.60.

(c) System compressor and turbine adiabatic efficiencies, 0.70

(d) System compressor and turbine adiabatic efficiencies, 0.80.

Figure 10. - Permissible auxiliary-compressor pressure ratio for free-running air-cycle refrigeration system. Heat-exchanger pressure ratio, 0.95.

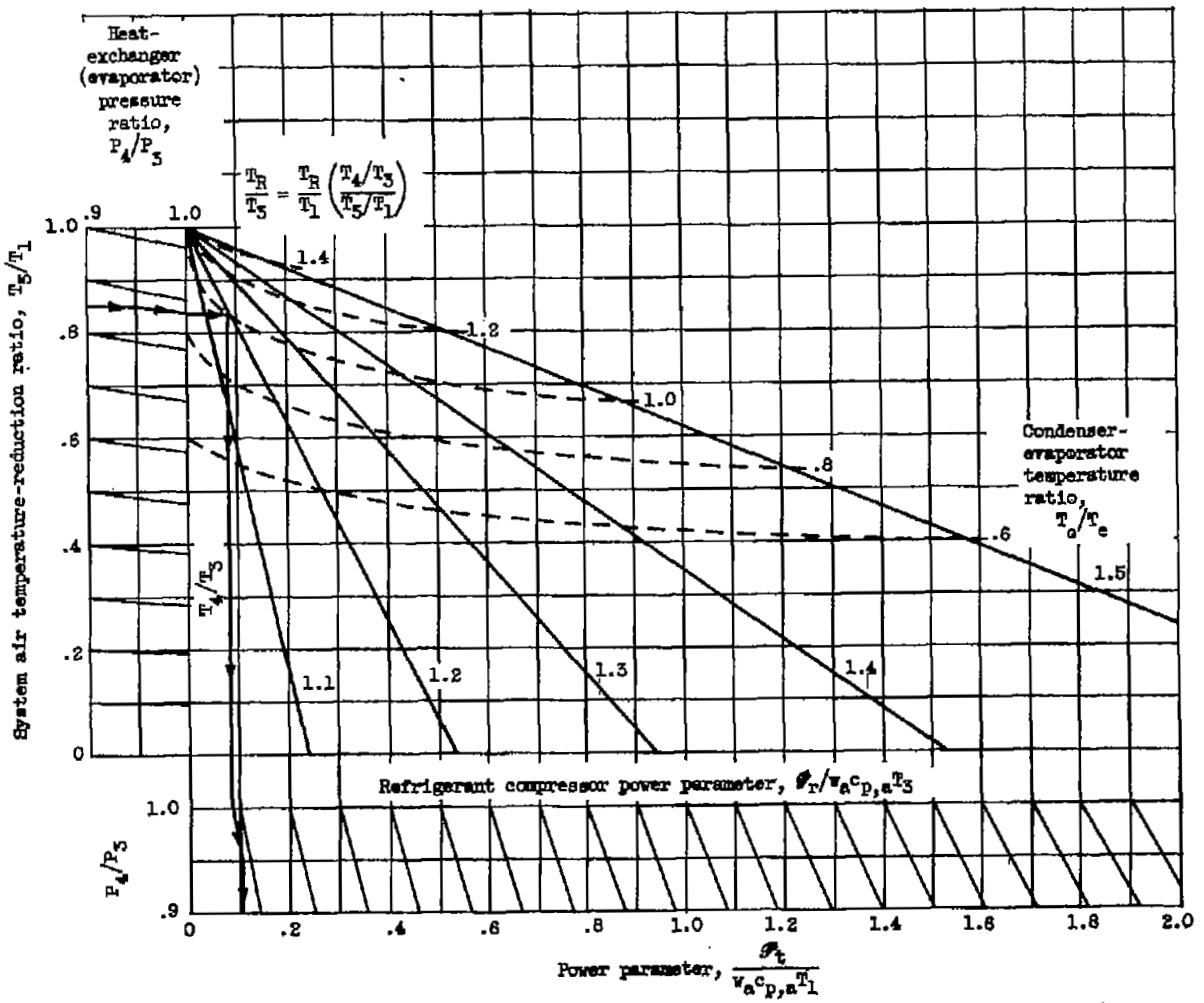

(a) Heat-exchanger (evaporator) effectiveness, 1.0; condenser effectiveness parameter, $\epsilon_c \frac{(wc_p)_R}{(wc_p)_a}$, ∞.

Figure 11. - Performance plot for mercury-vapor-cycle refrigeration system. Refrigerant compressor efficiency, 0.5; system air compressor adiabatic efficiency, 0.7; T_4/T_3, evaporator temperature-reduction ratio.

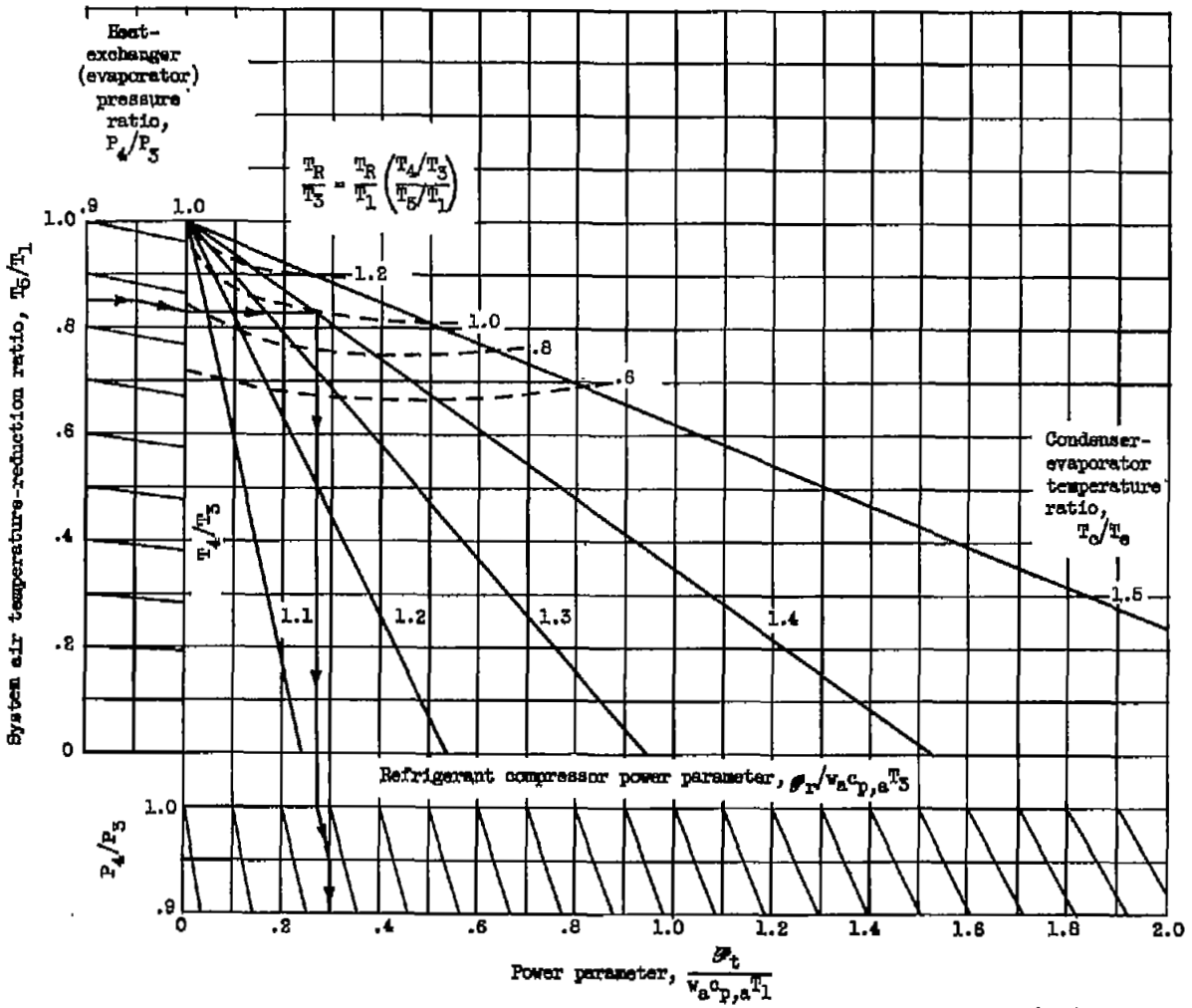

(b) Heat-exchanger (evaporator) effectiveness, 0.8; condenser effectiveness parameter, $\varepsilon_c \frac{(wc_p)_R}{(wc_p)_a}$, 4.

Figure 11. - Concluded. Performance plot for mercury-vapor-cycle refrigeration system. Refrigerant compressor efficiency, 0.5; system air compressor adiabatic efficiency, 0.7; T_4/T_5, evaporator temperature-reduction ratio.

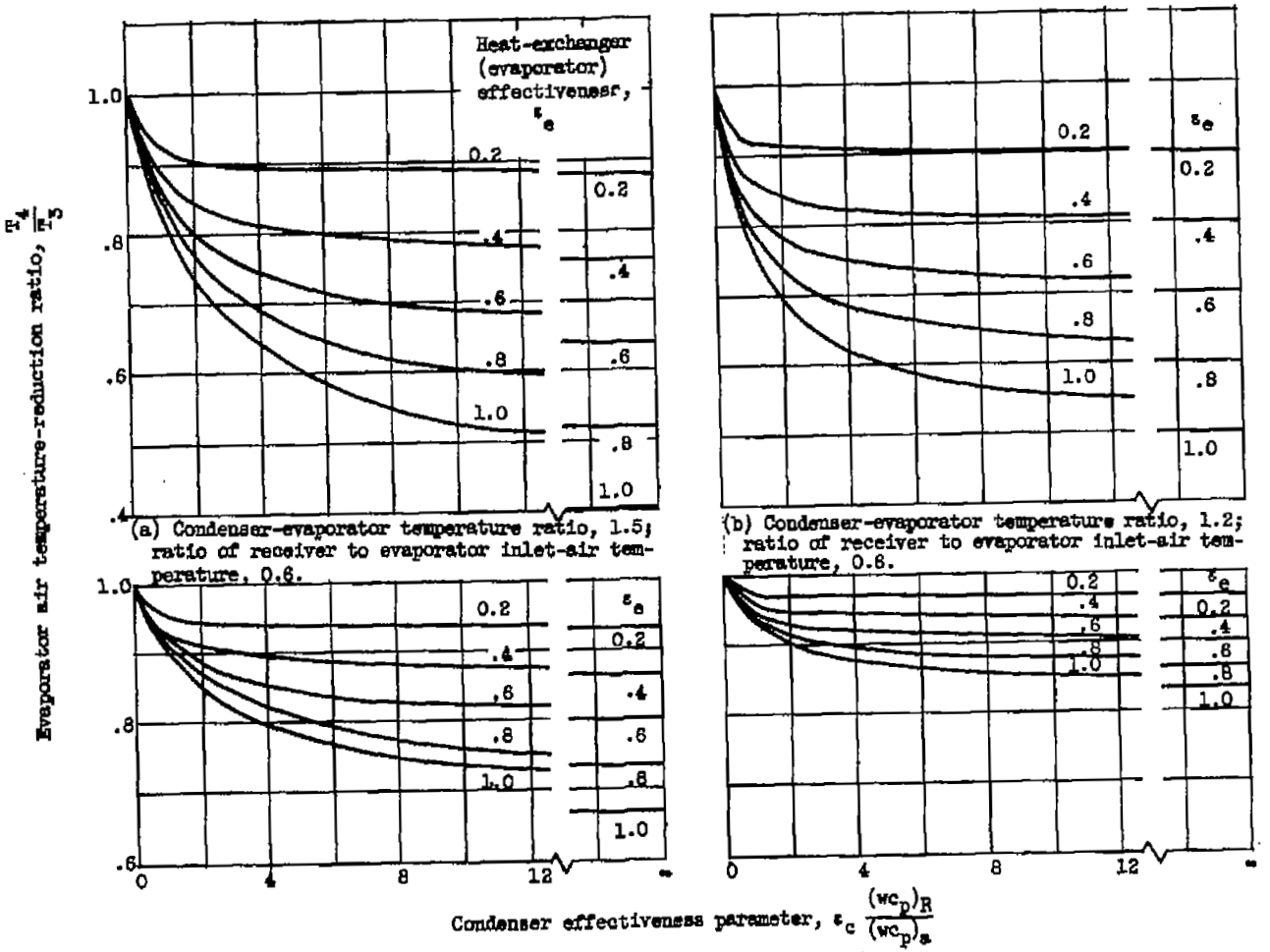

(a) Condenser-evaporator temperature ratio, 1.5; ratio of receiver to evaporator inlet-air temperature, 0.6.

(b) Condenser-evaporator temperature ratio, 1.2; ratio of receiver to evaporator inlet-air temperature, 0.8.

(c) Condenser-evaporator temperature ratio, 1.5; ratio of receiver to evaporator inlet-air temperature, 1.0.

(d) Condenser-evaporator temperature ratio, 1.2; ratio of receiver to evaporator inlet-air temperature, 1.0.

Figure 12. - Effect of condenser and evaporator effectiveness on mercury-vapor-cycle performance. Refrigerant compressor efficiency, 0.5.

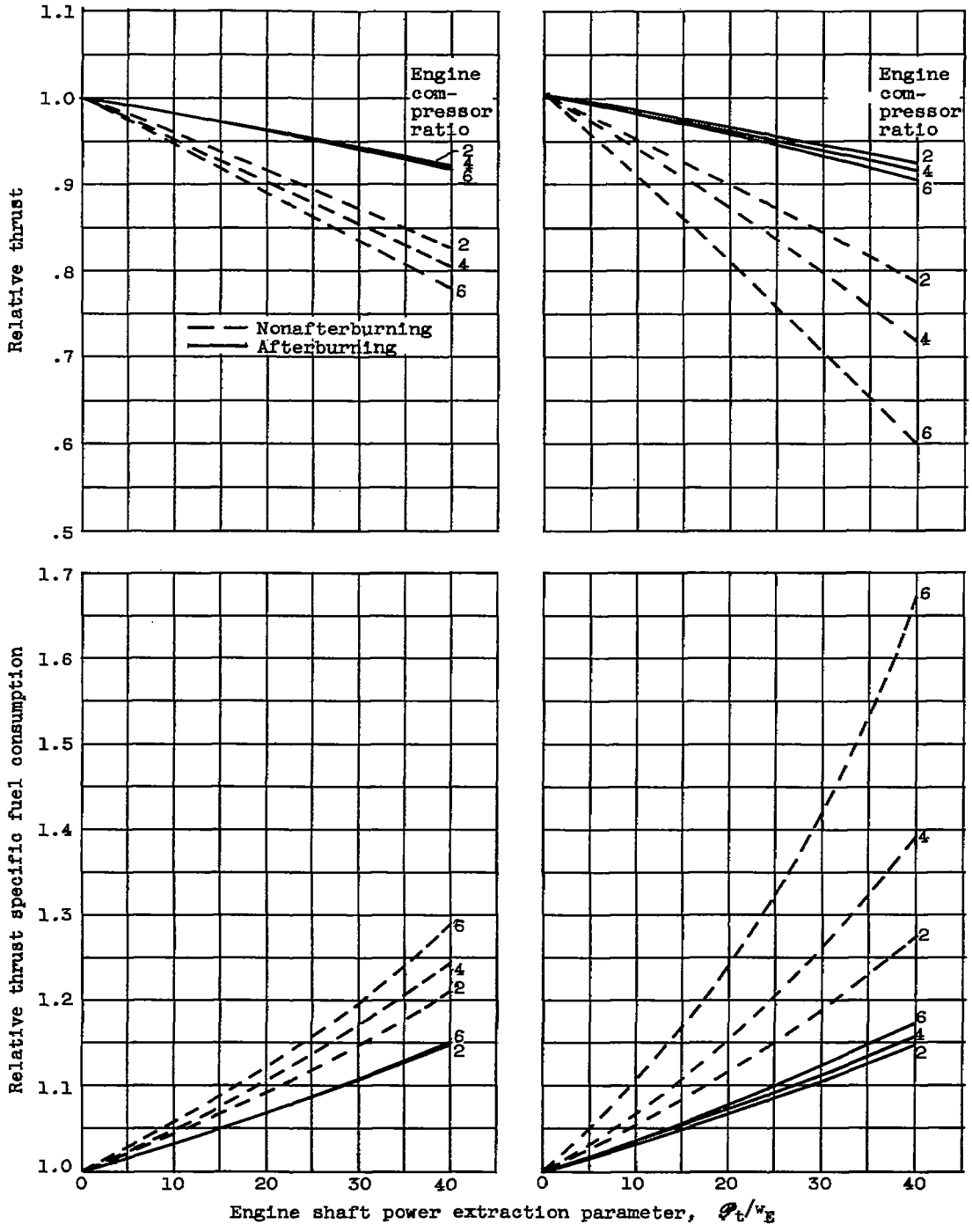

(a) Flight Mach number, 2.5 (b) Flight Mach number, 3.0.

Figure 13. - Effect of engine shaft power extraction on relative thrust and relative thrust specific fuel consumption.